U.S. DEPARTMENT OF THE INTERIOR

U.S. GEOLOGICAL SURVEY

Analysis of firn gases collected at shallow depths in the Wrangell-St. Elias range, Alaska, the GISP2 site, Greenland, and the Taylor Dome site, East Antarctica

by

Gary P. Landis[1], Joan J. Fitzpatrick[1], and T. Everett[2]

Open-File Report 95-222

[1] Denver, Colorado

[2] Claremont, California

1995

CONTENTS

	Page
Abstract	2
Introduction	3
Sampling and Analytical Procedures	4
Results	7
Wrangell-St. Elias, Alaska Study Area	7
GISP2 Summit, Greenland Study Area	10
Taylor Dome, Antarctica Study Area	21
Discussion	23
Conclusion	28
Future Research Directions	29
Acknowledgments	30
References	31
Appendix A. Analytical Methods and Calibration	A1
Appendix B. Sequencer Application for Routine Calibration and Analysis	B1

ILLUSTRATIONS

Figure 1.	Original firn gas probe design	5
Figure 2.	New firn gas probe design	5
Figure 3a.	Shallow firn gas ascent samples, nitrogen	9
Figure 3b.	Shallow firn gas ascent samples, oxygen	9
Figure 3c.	Shallow firn gas ascent samples, argon	9
Figure 3d.	Shallow firn gas ascent samples, carbon dioxide	9
Figure 3e.	Shallow firn gas ascent samples, δD	10
Figure 4a.	Depth profile for nitrogen in firn to 7.6 meters, Klutlan Glacier, Alaska	11
Figure 4b.	Depth profile for oxygen in firn to 7.6 meters, Klutlan Glacier, Alaska	11
Figure 4c.	Depth profile for argon in firn to 7.6 meters, Klutlan Glacier, Alaska	11
Figure 4d.	Depth profile for carbon dioxide in firn to 7.6 meters, Klutlan Glacier, Alaska	11
Figure 5a.	δD and snow density in 190 cm snow pit–4,420 meter col between Mt. Churchill and Mt. Bona, Alaska	12
Figure 5b.	δD and MSA in 190 cm snow pit–4,420 meter col between Mt. Churchill and Mt. Bona, Alaska	12
Figure 6.	GISP2 Summit site wind speed and direction, August 1992	13
Figure 7.	Comparison of wind speed, surface temperature, and station barometric pressure during firn gas sampling at GISP2	14
Figure 8a.	Depth profile for nitrogen in firn to 14.5 meters, GISP2, Greenland	15
Figure 8b.	Depth profile for oxygen in firn to 14.5 meters, GISP2, Greenland	15
Figure 8c.	Depth profile for argon in firn to 14.5 meters, GISP2, Greenland	15
Figure 8d.	Depth profile for carbon dioxide in firn to 14.5 meters, GISP2, Greenland	15
Figure 9a.	GISP2 depth profile–argon vs. nitrogen	16
Figure 9b.	GISP2 depth profile–argon vs. methane	16
Figure 9c.	GISP2 depth profile–methane vs. carbon dioxide	16

Page

Figure 10. Variations in "ground zero" surface CO_2 and temperature, GISP2, Greenland ---- 19
Figure 11. Variations in 3.0 meter deep CO_2, GISP2, Greenland ---- 19
Figure 12. Variations in 14.5 meter deep CO_2, GISP2, Greenland ---- 19
Figure 13. Variations in CO_2 showing time-space dependency resolved on a 24–hour sampling interval from the surface, 3.0 meters, and 14.5 meters depth in firn ---- 20
Figure 14a. Pumpdown experiment. Nitrogen change with continued pumping for 10 minutes. GISP2 ---- 21
Figure 14b. Pumpdown experiment. Oxygen change with continued pumping for 10 minutes. GISP2 ---- 21
Figure 14c. Pumpdown experiment. Argon change with continued pumping for 10 minutes. GISP2 ---- 21
Figure 14d. Pumpdown experiment. Carbon dioxide change with continued pumping for 10 minutes. GISP2 ---- 21
Figure 15. Firn gas composition depth profiles from adjacent 4.5-meter– and 10-meter–deep probes sampled under near identical weather conditions with exception of wind speed as noted in text. Taylor Dome, Antarctica ---- 22
Figure 16. Inverse relationship of nitrogen with carbon dioxide indicating variations in firn gas compositions are not a numerical artifact of analysis. Taylor Dome, Antarctica ---- 23
Figure 17. Dependence of average shallow firn gas carbon dioxide concentration on mean annual temperature of sites that range from sub–temperate, to polar, to extreme polar conditions of accumulation ---- 25

TABLES

Table 1. Churchill-Bona ascent δD and firn gas data, Alaska ---- 7
Table 2. Deep probe firn gas data, Alaska ---- 8
Table 3. Snow pit δD—MSA data, Alaska ---- 8
Table 4. GISP2 meteorologic conditions during sampling, August 1992 ---- 12
Table 5. GISP2 firn gas depth sampling profile, August 2, 1992 ---- 13
Table 6. GISP2 firn gas time series sampling: snow surface, August 7 through August 15, 1992 ---- 17
Table 7. GISP2 firn gas time series sampling: 3.0 meter depth, August 3 through August 15, 1992 ---- 17
Table 8. GISP2 firn gas time series sampling: 14.5 meter depth, August 3 through August 15, 1992 ---- 18
Table 9. GISP2 firn gas data: analysis of repeat samples ---- 18
Table 10. GISP2 firn gas pumpdown series sampling: 14.5 meter depth, August 12, 1992 ---- 19
Table 11. Taylor Dome, Antarctica, firn gas depth profile data ---- 22

Analysis of firn gases collected at shallow depths in the Wrangell-St. Elias range, Alaska, the GISP2 site, Greenland, and the Taylor Dome site, East Antarctica

by

G.P. Landis, J.J. Fitzpatrick, and T. Everett

Abstract

Analysis of shallow firn pore gas from the Wrangell-St. Elias range, Alaska, the GISP2 site in Greenland, and Taylor Dome site, Antarctica, indicates anomalous carbon dioxide contents 2x to 3x that of modern atmosphere. Average CO_2 enrichment of shallow firn gases shows a strong correlation with mean annual temperature of the field site, with low values of 710 ppmV and -45°C at Taylor Dome in Antarctica, and high values of 1,922 ppmV and -17°C on the Klutlan Glacier below Mt. Churchill and Mt. Bona in Alaska. Important selective wet deposition and in-cloud scavenging processes are indicated. This enriched carbon dioxide content is observed predictably in the relative solubility of carbon dioxide compared to nitrogen, oxygen, and argon in atmospheric water droplets. Very shallow firn pore spaces are dominated by air gases but in non-atmospheric concentrations. Recrystallization, sublimation, and densification of firn cause loss of this desorbed gas to voids and interstitial spaces. Below a depth of 15-20 meters, desorbing anomalous gas no longer dominates the composition of larger pore volumes but continues below this crossover point to exist in isolated micropores, grain boundaries, junctions, and crystal defect sites as "matrix" gas. The major permeability paths control exchange with the atmosphere and firn gas is like modern atmosphere in large interconnected pore spaces. Atmospheric gas transfer processes through the firn column to closure at the firn-ice transition include complex mixing and isolation of this anomalous gas with atmospheric gas. The likely persistence of this anomalous gas as matrix gas at depth complicates wet and dry extraction methods and interpretation of all ice gas data and clathrate behavior.

Introduction

The principal aim of the analysis of the CO_2 concentration in air extracted from ice-contained gas bubbles is to reconstruct the CO_2 concentration in the atmosphere during recent past climatic change. The implicit and critical assumption in studying the gas chemistry in ice core bubbles is that gases trapped in ice are direct samples of the atmosphere just prior to isolation of firn pore spaces in gas bubbles at the firn-ice transition. This assumption permits direct consideration of concentration levels of "greenhouse" gases in the atmosphere in comparison to various other indicators of changing climatic conditions (e.g. stable isotope data, accumulation rates). These data are used to reconstruct high-resolution paleoclimate records of recent past time (Stauffer, Neftel, and others, 1985; Wahlen, Allen, and Deck, 1991). However, this assumption may require some qualifications as transfer processes are investigated for atmospheric gases to ice core bubble volumes through a column of old snow or firn. Selective sorption and wet/dry deposition of gases in snow and firn diagenesis may significantly modify the concentration of minor gases like carbon dioxide from expected atmospheric levels. Both documented and suspected important transfer processes suggest that the entrapment of atmospheric gases in ice gas bubbles is very complex (Colbeck, 1989; Craig, Horibe, and Sowers, 1988; Gedzelman and Arnold, 1994; Jaworowski, Segalstad, and Hisdsal, 1992; Martinerie, Raynaud, and others, 1992; Nakazawa, Machida, and others, 1993; Schwander, Barnola, and others, 1993; Sowers, Bender, and Raynaud, 1989; Zumbrunn, Neftel, and Oeschger, 1982). We have designed a probe capable of sampling firn gases to approximately 15 meters depth. Samples were collected within several experimental frameworks from the Klutlan Glacier, and Mt. Churchill and Mt. Bona of the Wrangell-St. Elias range, Alaska, the GISP2 ice core drill site, Greenland, and the Taylor Dome drill site, East Antarctica. Experimental sampling was designed to test the nature of carbon dioxide transfer from the atmosphere through the firn column to discrete ice-enclosed gas bubbles. This study is capable only of investigating shallow atmosphere–firn processes, lacking the ability to penetrate the firn column to the firn–ice transition (typically >50 to 150 meters depth depending upon site). Deeper

sampling access requires coring or drilling equipment and additional constraints on the validity of samples taken. Research efforts not reported here include development of a laser microbeam-mass spectrometer system to analyze individual gas bubbles in ice cores across the firn-ice transition and to greater depths to investigate possible heterogeneity and modifications to gas chemistry of gases in ice with closure and compaction of pore volumes and recrystallization of ice fabric. This new analytical procedure may better constrain air-ice age differences and aid in interpreting greenhouse gas composition data. These combined studies will address the validity of ice core gas data and the limitations of interpretation that can be expected given a better understanding of relevant transfer processes and modifications that occur to gases in ice.

Sampling and Analytical Procedures

Details of analytical methods, including instrumentation, data collection and reduction, and calibration, accuracy, and precision are given in the appendices to this report. All instrument development and sample analyses were completed at the U.S. Geological Survey stable isotope-gas geochemistry laboratory in Denver, Colorado. Samples were collected for analysis in untreated 10 ml glass vacutainer vials via the firn gas probes described below during field seasons to the Wrangell-St. Elias range, Alaska (May-June 1992), GISP2 site in Greenland (August 1992), and the Taylor Dome site, Antarctica (January 1993). Sample analyses were completed in late 1994, after testing and calibration of instrumentation. The analytical method described in Apendix A of this report yields a typical analytical precision for "air" gases at one sigma standard deviation of N_2 (± 0.015 percent), O_2 (± 0.014 percent), Ar (± 17.6 ppmV) and CO_2 (± 0.72 ppmV) based upon repeat analysis of NIST traceable standard reference gas. Analysis of CH_4 and N_2O could not be performed without prior separation on a gas chromatographic column because of ^{15}N and H_2O interference on AMU 15 and 16, respectively for methane, and $N_2 - CO_2$ and $^{15}N - ^{18}O$ interference on AMU 30 and 44 for nitrous oxide. With completion of a GC column and jet separator inlet, future analyses will include these species.

The firn gas probe uses 1.5 meter sections of 5/8" x 1/2" stainless steel pipe fitted with threaded ends for assembly to a continuous hollow length, with a side hole pointed end attached to the first section. Figure 1 illustrates the original probe valve design used to collect the Alaskan and Greenland samples. An improved valve block design (fig. 2) modification was utilized in collecting the Antarctic Taylor Dome samples. The probe is driven into the firn with a new section of pipe attached as required until the maximum penetration depth (typically 10-15 meters deep) is reached by pounding the fitted end cap with a sledge. Before each new section of pipe is added, a sample of firn pore gas is pumped from the penetration depth through the probe and collected. Sampling consists of both purge pumping the pipe sections to obtain representative samples from the probe point depth, and repeatedly purging the vacutainer vial with sample gas prior to taking a sample. A teflon-viton diaphram pump operated with a 12 volt dc gel cell battery and capable of approximately 2 l/m capacity pumped gases through the probe for 4 minutes before a sample was taken. At a maximum depth of 14.5 meters obtained for the GISP2 site, an internal volume of probe pipe sections was 1.25 liters. A net drawdown of 6.75 liters at the probe point was achieved prior to sampling. This is

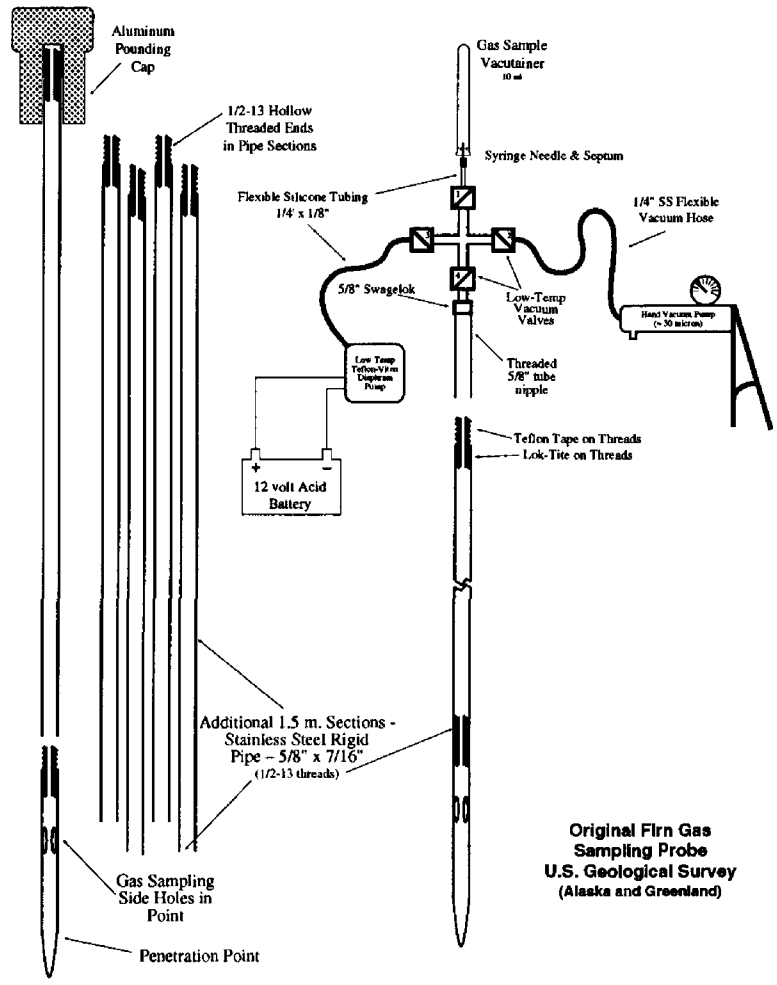

Figure 1. Original firn gas probe design.

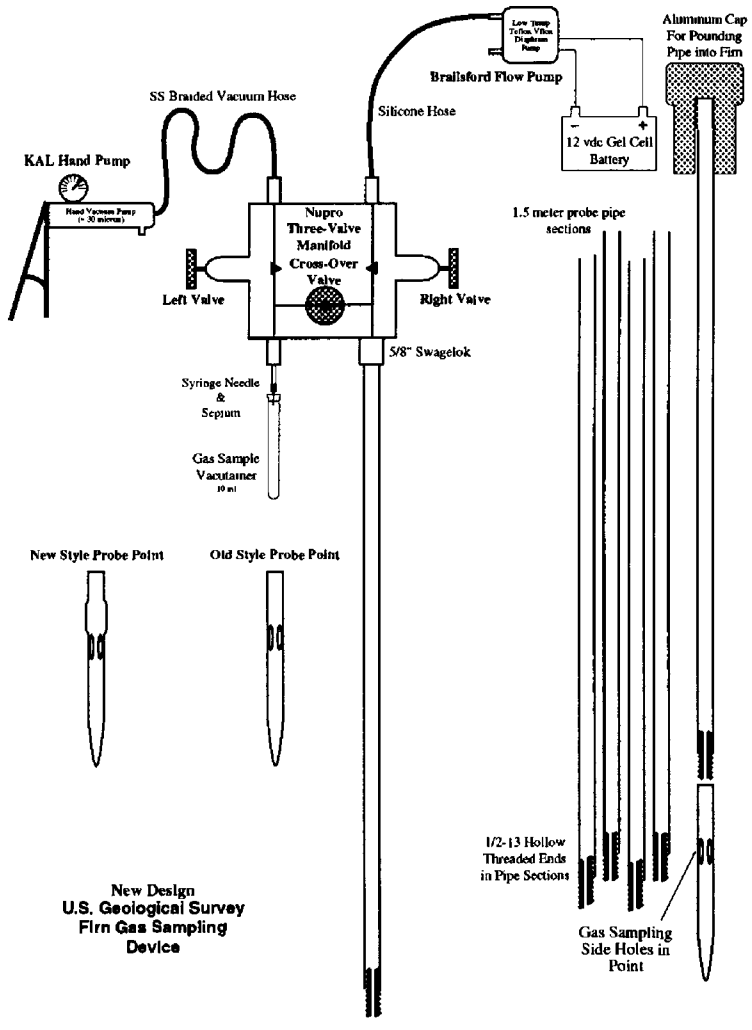

Figure 2. New firn gas probe design.

compared to the vastly greater volume throughput used by Bender and others (1994), and Schwander and others (1993) of >500 liters and ≈ 10,000 liters, respectively. We speculate, in discussion below, that this greater throughput of firn pore gases makes results of these other researchers impossible to compare with our own. We suggest that our minimal gas drawdown prior to sample collection yields a pore gas more representative of that actually in the firn.

Vacutainer vials were evacuated with a dry hand pump to ≈ 30 microns pressure, backfilled with gas from the drawdown flow, and again evacuated a total of three times prior to taking a sample at 4 minutes of pumping. This purges the vacutainer vial of all contaminants and assures a representative gas sample. With the firn gas sample loaded at ambient site barometric pressure, the needle was withdrawn from the septum and the vial marked for analysis. Unfortunately, because of elevation and air mass temperature–density at the three sites sampled, the internal pressure of vacutainers is slightly less than that of ambient air in Denver (approximately 20 percent less). However, no special precautions to seal the punctured septum were indicated as prior experiments with helium standards indicated vacutainers were capable of preserving helium sample integrity for more than 8-10 months (I. Friedman, oral commun., 1992). Vacutainer sample integrity has been verified by repeat analysis of both standard reference air and Denver urban air samples collected and held in untreated Vacutainer vials for several months.

Several sampling experiments were conducted using the firn gas probe described. At each site a depth profile of firn gas compositions was determined by samples taken as each section of stainless steel pipe was added and a deeper probe penetration achieved. A depth of 7.6 meters was attained for the site on the Klutlan Glacier, Alaska. Probes were placed to a depth of 14.5 meters and 3.0 meters for the GISP2 site, and 4.5 meters and 10.0 meters for the Taylor Dome site. After emplacement of the GISP2 site probes, a daily time series sample was taken at 24-hour increments from both 14.5 meters and 3.0 meters depth and at "ground zero" surface. Also, a series of samples were taken from the 14.5 meter probe at GISP2 as a function of pumping time or drawdown. In addition to the firn probe samples taken at the Alaska site, a

series of 1.0 meter and 1.5 meter depth snow gas sample pairs were taken during the ascent from the drop point on the Klutlan Glacier (3,200 meter elevation) to base camp in the col between Mt. Churchill and Mt. Bona (4,300 meter elevation) using a 1.5 meter long 1/4" diameter soil gas sampling probe and the vacutainer loading procedures described above.

In the Results and Discussion sections of this report, gases analyzed are collectively referred to as "air" gases meant to include the standard atmospheric gases nitrogen (in percent volume), oxygen (in percent volume), argon (in percent or ppmV), and carbon dioxide (in percent or ppmV). These data also can be considered in equivalent units of mole fractions or partial pressures. Modern atmospheric gas composition is N_2 = 78.04 percent, O_2 = 20.99 percent, Ar = 9340 ppmV, and $CO_2 \approx$ 360 ppmV. Methane is about 1,600 ppbV and nitrous oxide is 200-300 ppbV, though we cannot precisely measure these last two components at this time.

Results

Wrangell-St. Elias, Alaska Study Area — Firn gas samples were collected as part of an initial site survey in 1992 on the Klutlan Glacier and Mt. Churchill and Mt. Bona in the Wrangell-St. Elias range of Alaska. Site characterization on the glacier and in the col between Mt. Churchill

Table 1. Churchill-Bona ascent δD and firn gas data (shallow probe samples).

Elevation (m)	δ D (smow) (permil)	N_2 (mole %)	O_2 (mole %)	Ar (mole %)	CO_2 (mole %)
Surface Snow and 1.0 meter firn gas samples					
3200	-227	- - -	- - -	- - -	- - -
3301	-238	78.283	20.563	1.005	0.148
3432	-232	77.507	21.276	1.049	0.168
3548	-226	78.185	20.564	0.982	0.270
3597	-159	79.768	19.151	0.999	0.082
3719	-223	78.385	20.532	1.008	0.075
3810	-178	78.926	20.009	0.978	0.087
3993	-294	77.631	21.148	0.979	0.241
4084	-288	77.865	21.068	0.985	0.082
4185	-282	77.343	21.541	1.025	0.090
4298	-279	77.220	21.627	1.018	0.135
0.5 meter Snow and 1.5 meter firn gas samples					
3200	-216	78.205	20.658	1.036	0.101
3301	-204	78.483	20.398	1.024	0.095
3432	-175	77.877	20.883	0.994	0.245
3548	-185	79.293	19.645	0.950	0.113
3597	-208	78.324	20.588	1.057	0.031
3719	-224	78.899	20.022	0.999	0.079
3810	-212	78.221	20.673	1.009	0.096
3993	-206	79.433	19.533	0.964	0.070
4084	-209	77.680	21.230	0.999	0.091
4185	-235	77.993	20.950	0.949	0.108
4298	-170	77.567	21.314	0.981	0.138

and Mt. Bona are summarized by Landis and others (1993), Hinkley and others (1991), and Fitzpatrick and others (1992). A total of 21 shallow probe snow gas samples at 1.0 meter and 1.5 meter (table 1) depths was taken on the ascent from 3,200 meters on the Klutlan Glacier to

Table 2. Deep probe firn gas data (elevation 3,200 meters).

Depth (meters)	N_2 (mole %)	O_2 (mole %)	Ar (mole %)	CO_2 (mole %)
0.00	74.678	24.080	1.095	0.147
1.52	77.659	21.119	0.992	0.230
3.05	77.646	21.117	0.956	0.281
4.57	76.990	21.868	0.967	0.175
6.10	77.265	21.514	1.019	0.203
7.62	78.139	20.779	0.964	0.117

base camp in the col between Mt. Churchill and Mt. Bona at 4,300 meters, 6 samples were obtained from the depth profile to 7.6 meters depth at the 3,200 meter elevation camp (table 2), and snow was collected at each elevation for δ D analysis. MSA and δ D analyses were

Table 3. Snow pit δ D — MSA data (near col base camp at elevation 4,298 meters).

Depth Interval (inches)	Depth (cm)	δD (permil)	MSA (ppb)
0-5	12.7	- 292	5
5-10	25.4	- 218	3
10-15	38.1	- 218	3
15-20	50.8	- 179	2
20-25	63.5	- 217	2
25-30	76.2	- 243	2
30-35	88.9	- 190	11
35-40	101.6	- 167	8
40-45	114.3	- 170	2
45-50	127.0	- 178	3
50-55	139.7	- 175	1
55-60	152.4	- 181	2
60-65	165.1	- 170	5
65-70	177.8	- 178	2
70-75	190.5	- 157	6

performed for 15 samples from a shallow 190 cm snow pit at the col base camp to characterize seasonal variations (table 3). Results of these first studies suggested to us that the gas transfer processes between atmosphere and gas bubbles in ice through the firn column might be more complex than suspected. Figure 3 a-d illustrates the variation in shallow firn atmospheric gases

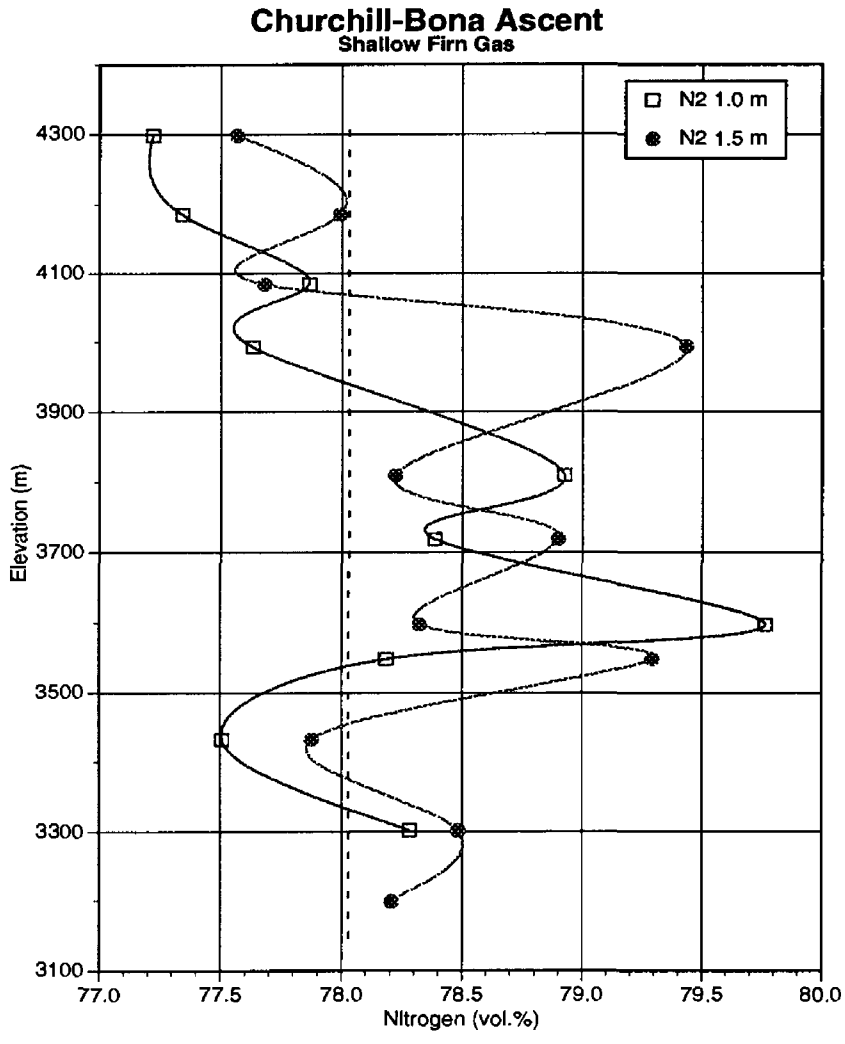

Figure 3a. Shallow firn gas ascent samples–nitrogen (percent).

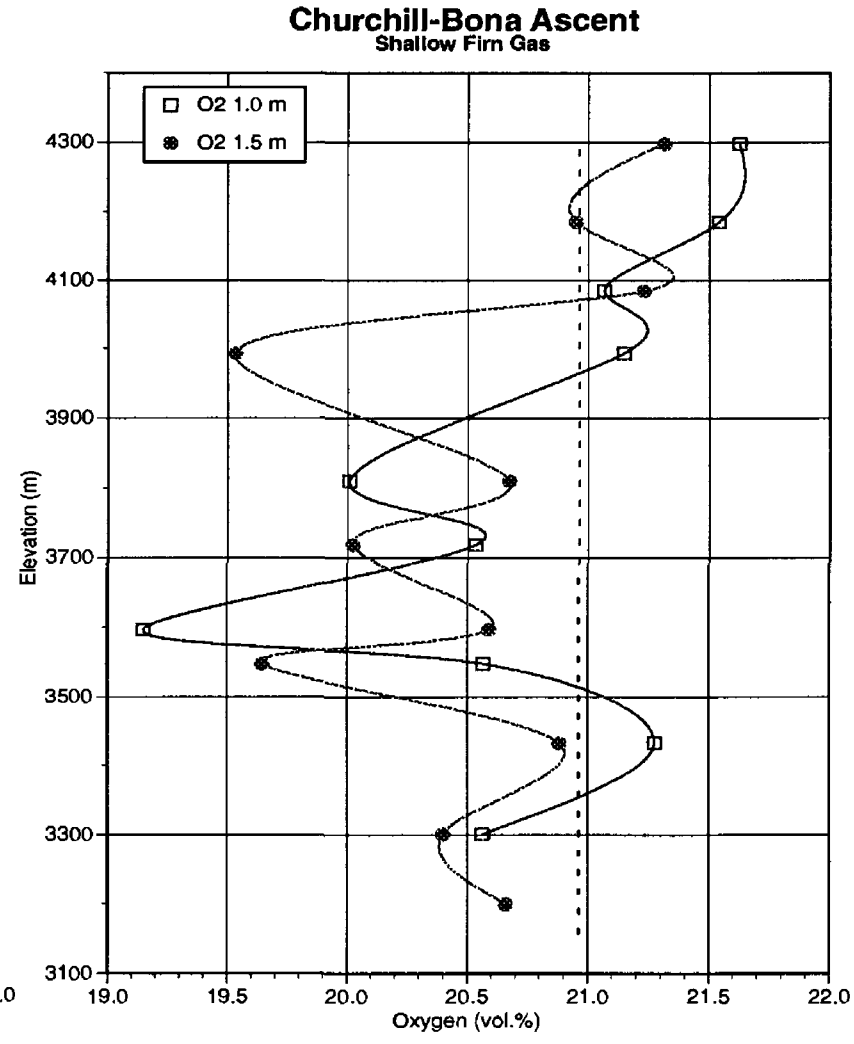

Figure 3b. Shallow firn gas ascent samples–oxygen (percent).

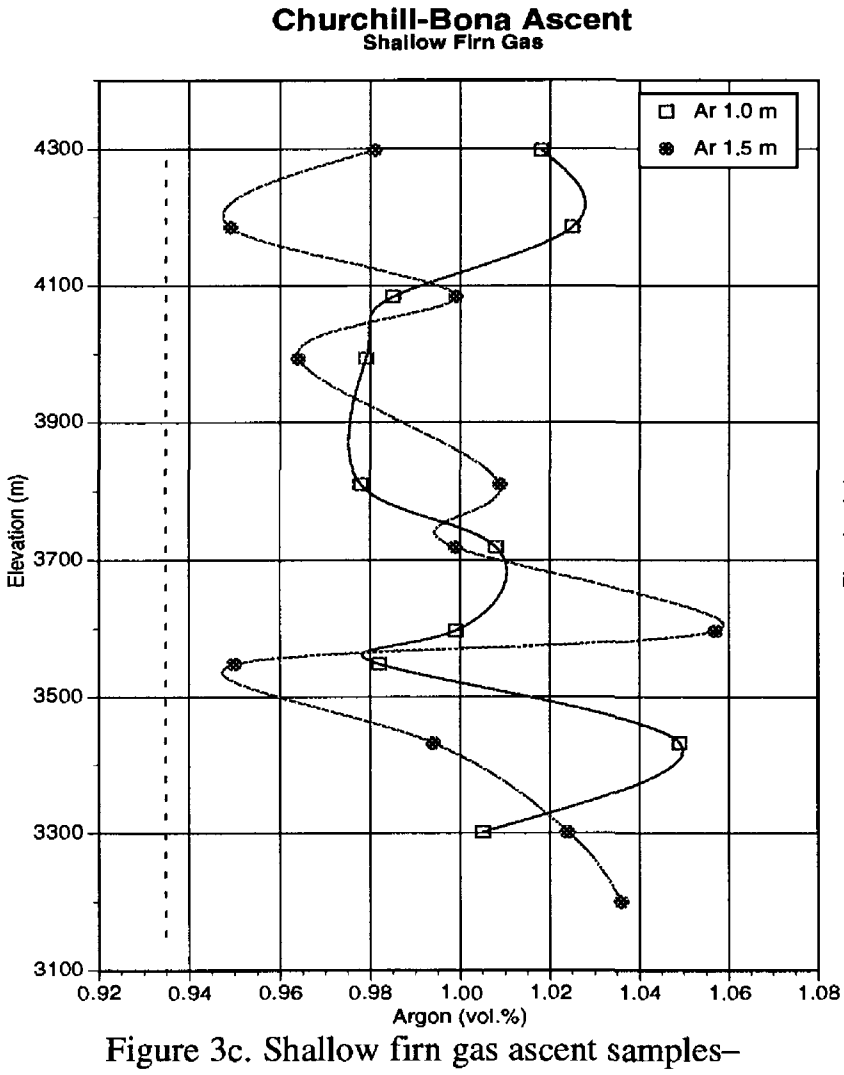

Figure 3c. Shallow firn gas ascent samples–argon (ppmV).

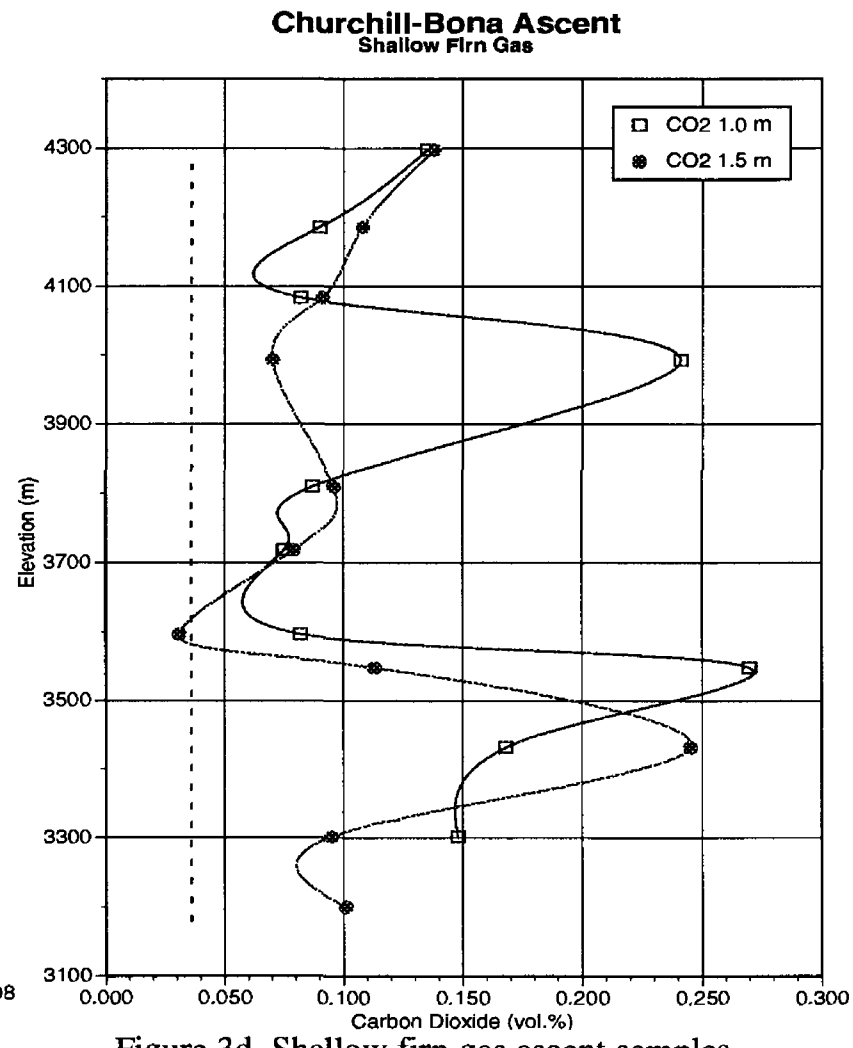

Figure 3d. Shallow firn gas ascent samples–carbon dioxide (ppmV)

with elevation on the Klutlan Glacier. An average CO_2 is nearly 1,100 ppmV with the 1.0 meter depth generally elevated compared to the 1.5 meter depth, and with covariation of both values. Figure 3 e illustrates the δ D of snow collected at each shallow firn ascent sample site from the surface and from a depth of 0.5 meters. The more variable surface δ D_{snow} shows the input from individual storm events that is isotopically smoothed in the 0.5 meter δ D_{snow}. Firn gas composition as a function of depth (fig. 4 a-d) is clearly not atmospheric, but appears to converge to "air-like" values with depth (possibly 10-15 meters). Carbon dioxide

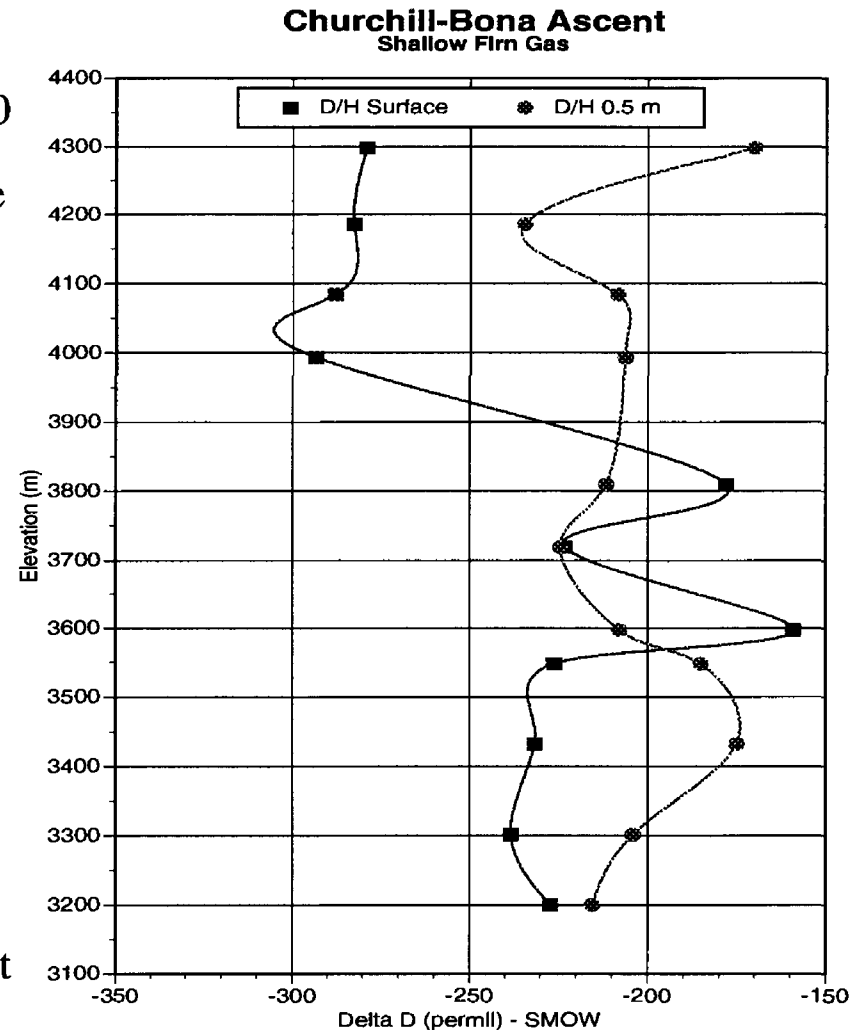

Figure 3e. Shallow firn gas ascent samples– δ D (permil) SMOW.

exhibits a high value of 2,800 ppmV and a low of 1,170 ppmV. Snow pit data are plotted in Figure 5a - 5b. Density and δ D versus depth show only a seasonal trend and increasing density of snow with depth. Methanesulfonic acid (MSA) and δ D data indicate a clear inverse seasonal signal, with lower δ D (colder temperature) corresponding to nearly a 10-fold increase in MSA. These spikes correspond in time with the late spring breakup of northern arctic ice and the opening of arctic waters. We speculate that these data record a shift in air mass circulation from winter Aleutian weather fronts to that of spring arctic fronts.

GISP2 Summit, Greenland Study Area —Sampling at the GISP2 Summit site (Grootes, Stuiver, and others, 1993) was designed as an extracurricular test study and was not part of the official GISP2 project. All firn gas samples were taken August 2 through August 15, 1992. Prevailing meteorological conditions are summarized in table 4 and plotted in figures 6 and 7. Changing weather conditions at the probe sampling site are recorded in air temperature (°C), wind speed (knots), and station barometric pressure (mbar). On August 2, 1992, the firn probe

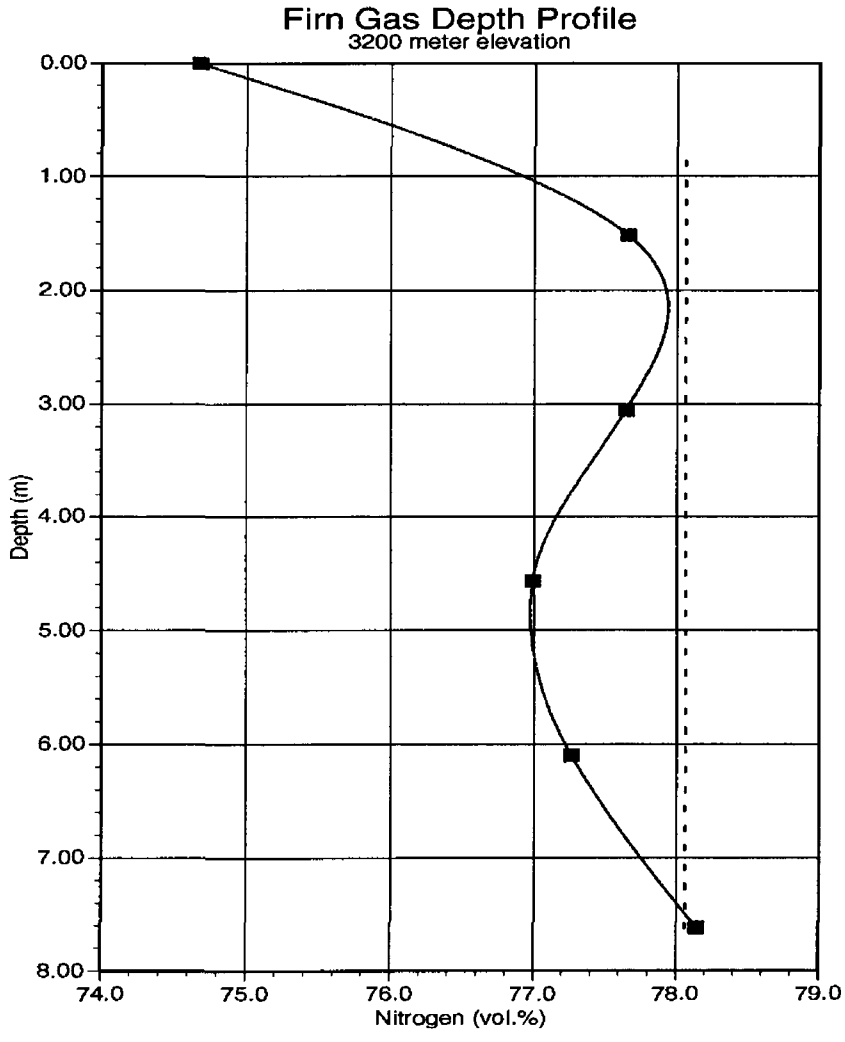

Figure 4a. Depth profile for nitrogen in firn to 7.6 meters, Klutlan Glacier, Alaska.

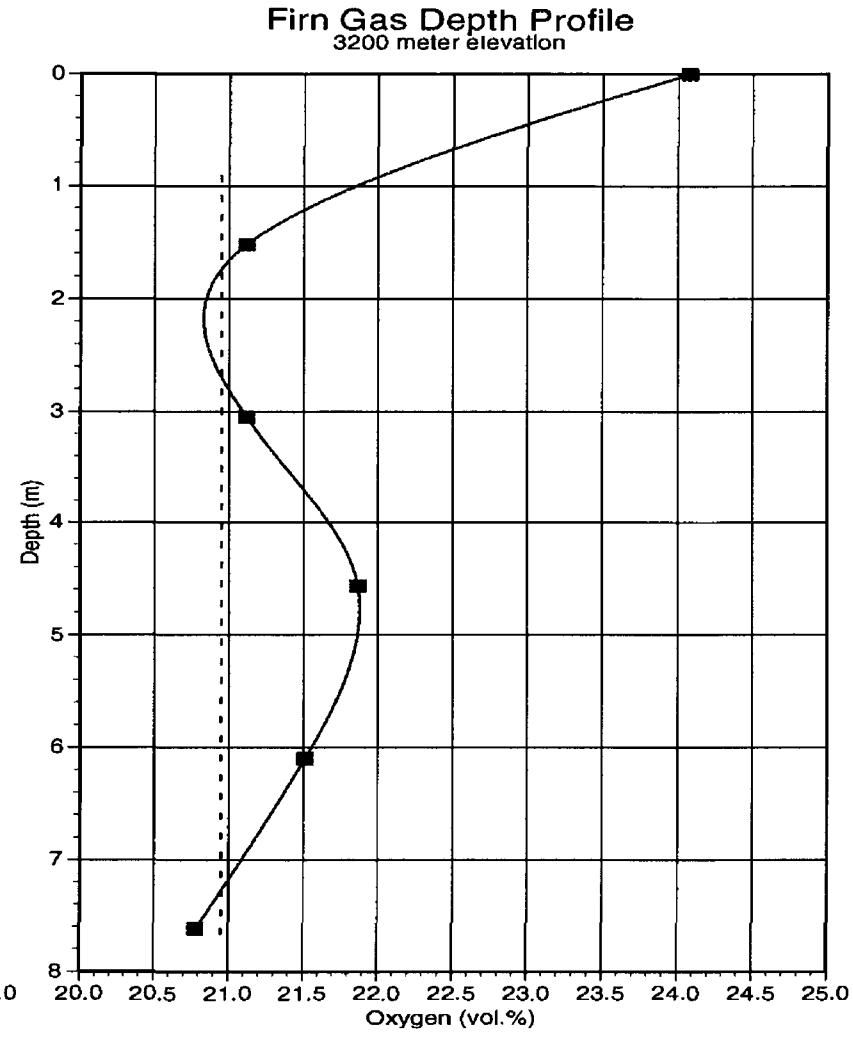

Figure 4b. Depth profile for oxygen in firn to 7.6 meters, Klutlan Glacier, Alaska

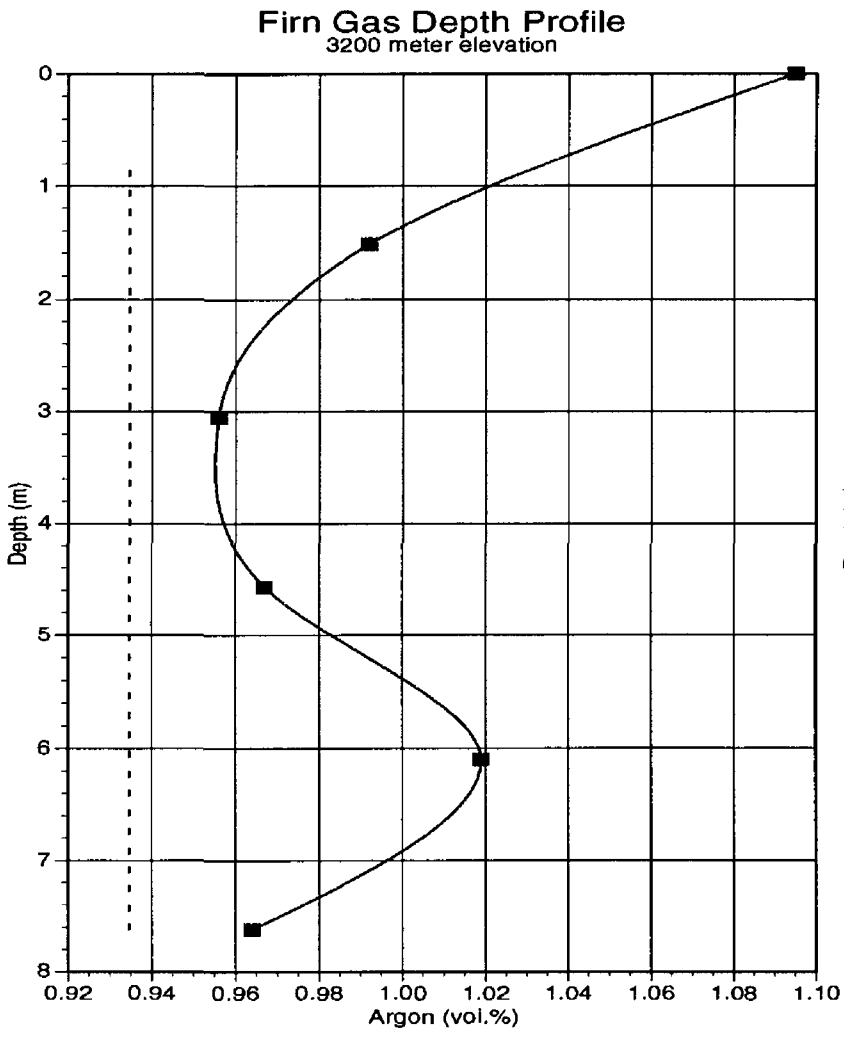

Figure 4c. Depth profile for argon in firn to 7.6 meters, Klutlan Glacier, Alaska.

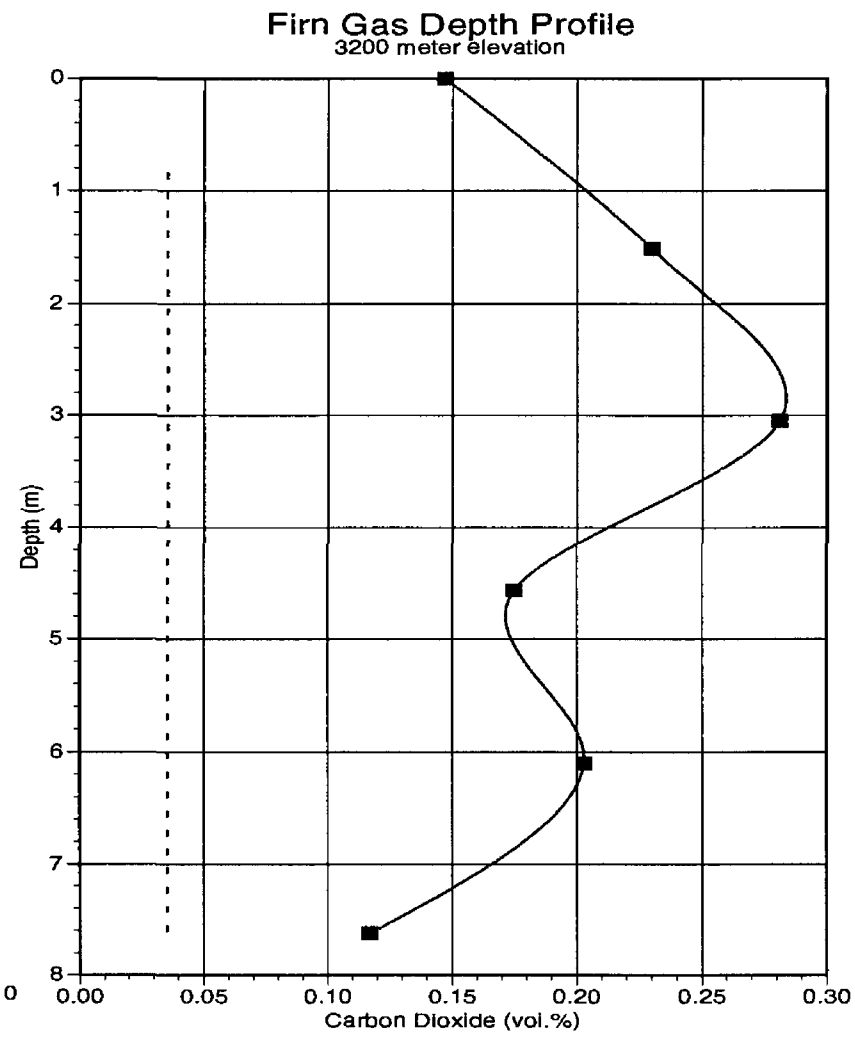

Figure 4d. Depth profile for carbon dioxide in firn to 7.6 meters, Klutlan Glacier, Alaska.

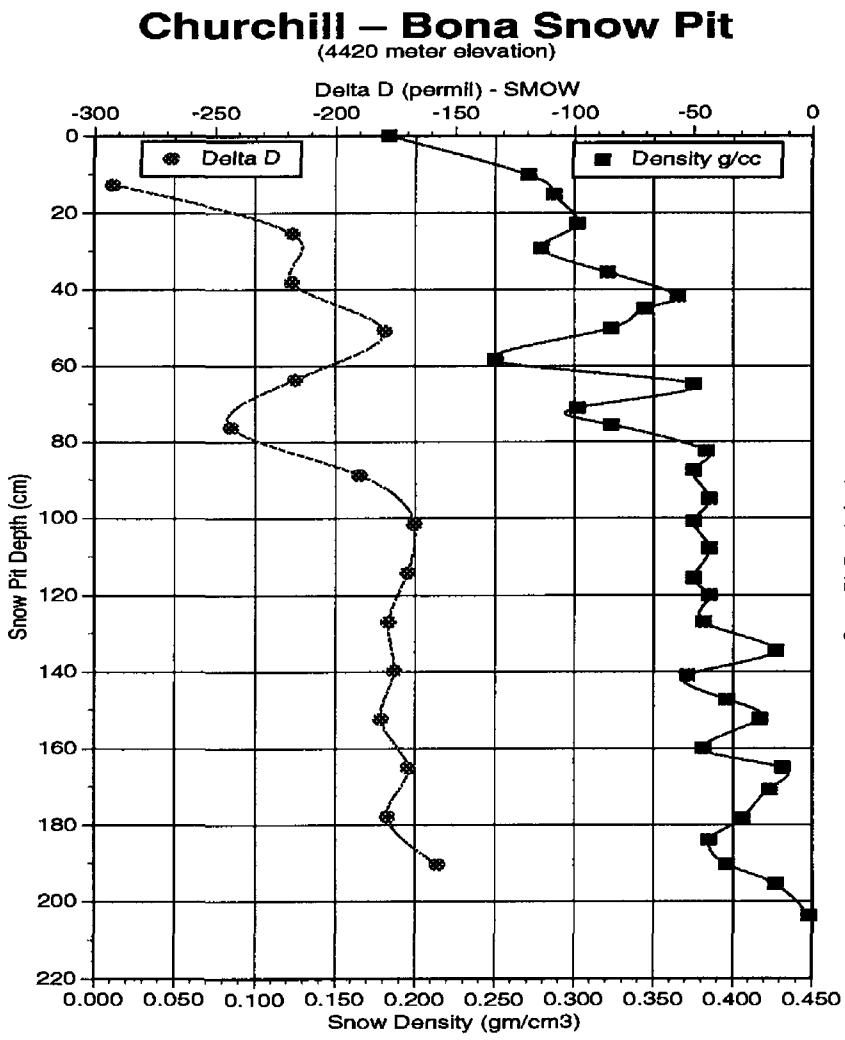

Figure 5a. δD and snow density in 190 cm snow pit—4,420 meter col between Mt. Churchill and Mt. Bona, Alaska.

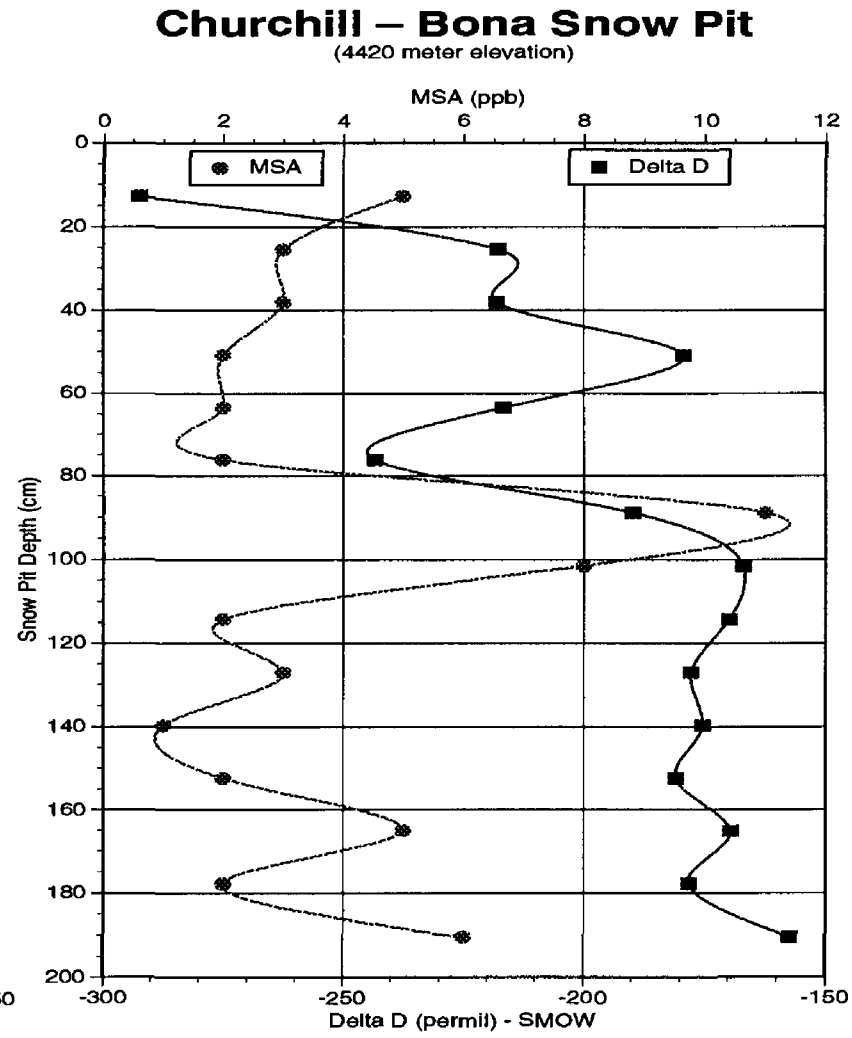

Figure 5b. δD and MSA in 190 cm snow pit—4,420 meter col between Mt. Churchill and Mt. Bona, Alaska.

was placed to a depth of 14.5 meters during a 5:45 hour interval, collecting 13 samples at measured depths (table 5). These data are plotted (fig. 8 a-d) against depth and exhibit large variations in gas compositions. Surface CO_2 is nearly 600 ppmV and varies between 382 and 706 ppmV. Data trends suggest that firn gas compositions possibly approach that of atmosphere at greater depths (15-20 meters). Though our methods cannot analyze methane and nitrous

Table 4. GISP2 meteorologic conditions during sampling, August 1992.

Date	Start-hrs	Stop-hrs	Lapsed Time	Air Temp °C	Dew Point °C	Barometric Pressure mbar	Wind Speed knots	Wind Direction	Remarks
8/2/92	08:45 AM	02:30 PM	05:45	- 17.0	- 24	1002.7	3	230°	10 yds W (upwind) of Sowers' 4" hole-clear, BP falling
8/3/92	10:30 AM	12:00 PM	01:30	- 10.0	- 18	998.1	17	250°	overcast, snowing
8/4/92	09:00 AM	09:45 AM	00:45	- 15.0	- 26	997.4	4	220°	skies dense, low overcast
8/5/92	09:20 AM	10:05 AM	00:45	- 15.0	- 25	995.2	8	280°	mostly clear, light high overcast
8/6/92	10:15 AM	10:45 AM	00:30	- 12.0	- 28	999.5	6	290°	skies clear
8/7/92	09:15 AM	10:00 AM	00:45	- 23.0	- 32	996.5	8	340°	skies overcast
8/8/92	08:00 AM	08:45 AM	00:45	- 14.0	- 20	1001.2	3	140°	low overcast to broken clouds
8/9/92	11:05 AM	11:40 AM	00:35	- 7.0	- 16	1007.0	10	350°	overcast and snowing
8/10/92	08:15 AM	08:50 AM	00:35	- 18.0	- 23	1006.4	1	110°	skies clear
8/11/92	09:00 AM	09:26 AM	00:26	- 16.1	- 24	1003.1	3	250°	changing to dense fog, warming rapidly - below freezing
8/12/92	09:05 AM	09:34 AM	00:29	- 18.0	- 24	1000.6	1	100°	heavy fog, clearing at end of sampling-PumpTest
8/13/92	08:45 AM	09:10 AM	00:25	- 22.1	- 28	998.1	2	150°	skies clearing in light fog, riming in evening
8/14/92	09:45 AM	10:12 AM	00:27	- 17.0	- 22	997.2	1	196°	grnd fog, clearing to blue skies, warming, heavy hoar
8/15/92	09:00 AM	09:30 AM	00:30	- 20.0	- 25	995.4	11	140°	overcast, light ground fog.

Table 5. GISP2 firn gas depth sampling profile, August 2, 1992.

Sample Name	Depth meters	Nitrogen %	Oxygen %	Argon ppm	Carbon Dioxide ppm
Depth-1	-1.00	74.8205	21.8232	9309.4	593.93
Depth-2	0.00	73.0165	21.7823	9303.4	601.83
Depth-3	0.76	75.2056	22.0169	9398.1	504.71
Depth-4	1.52	74.5042	21.6171	9426.9	477.01
Depth-5	3.05	72.5817	21.9707	9321.1	584.35
Depth-6	4.57	75.7560	21.5719	9419.4	483.28
Depth-7	6.10	77.2053	21.8898	9481.7	419.22
Depth-8	7.62	75.1735	21.7909	9439.9	463.12
Depth-9	9.14	76.6123	21.8934	9469.7	431.75
Depth-10	10.67	74.9563	21.7981	9411.7	491.57
Depth-11a	12.19	75.3635	21.5484	9334.0	569.07
Depth-12a	13.72	68.6111	21.2868	9204.4	705.75
Depth-13a	14.48	77.9470	22.0074	9518.3	381.77

oxide reliably (≈ 10 percent error) without GC column separation (because of isotopic mass interference), the depth profile series included both methane and nitrous oxide for comparison. These data are plotted to test variations in these minor to trace atmospheric components and to determine if air components of lesser concentration were numerically varying only in response to minor analytical variations in major nitrogen and oxygen. Argon shows an inverse relationship to nitrogen (fig. 9 a), yet exhibits a positive correlation to methane (fig. 9 b).Thus, methane concentration is not dependent upon minor variations in nitrogen or ^{15}N. Methane and carbon dioxide show a positive covariance (fig. 9 c). The fact that a 1 percent level argon component is inverse to a 78 percent nitrogen while exhibiting a positive relationship to 1,600 ppb level methane, and methane and 360 ppm level carbon dioxide covariance is significant, requires the observed carbon dioxide variations be "real" and not an analytical artifact.

Upon completing the depth profile firn gas sampling to the maximum penetration depth, an additional probe was placed to a depth of 3.0

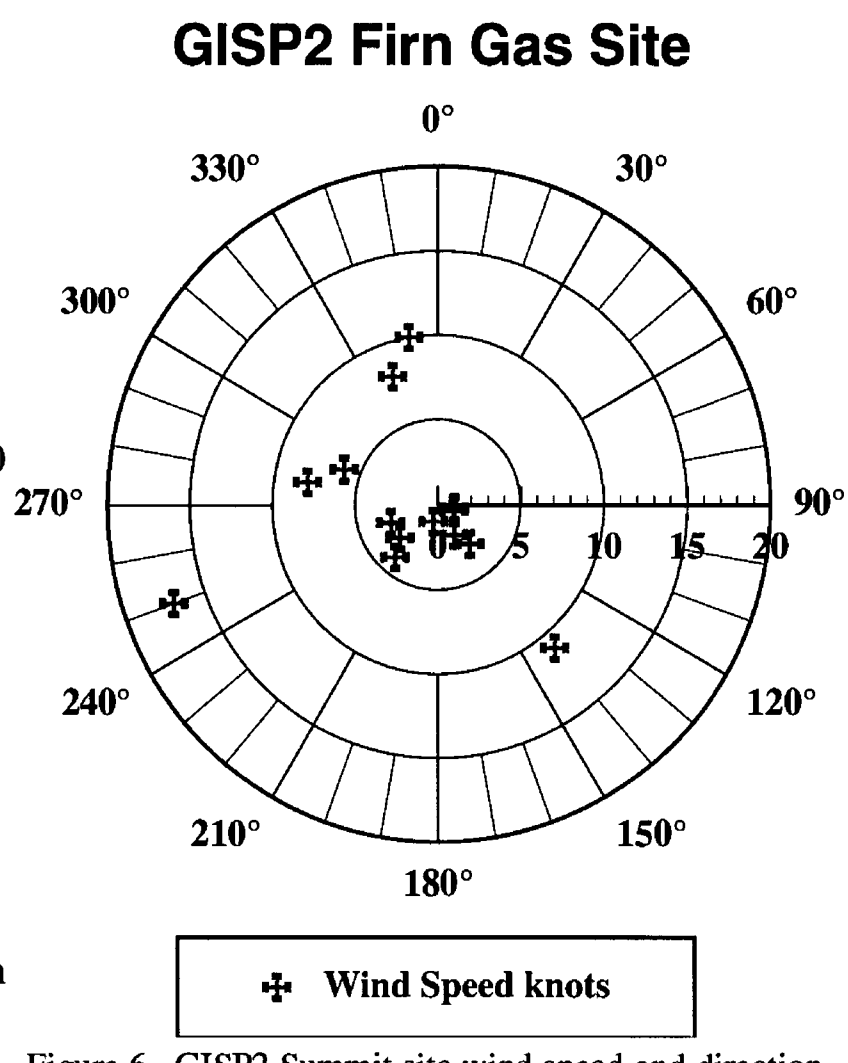

Figure 6. GISP2 Summit site wind speed and direction, August 1992.

meters approximately one meter distance from the 14.5 meter probe. At approximately 9:30 a.m. on each of the following days of sampling (August 3 through August 15), a suite of samples were collected at the surface (table 6), at 3.0 meters (table 7), and at 14.5 meters (table 8) depth, to establish a time series of firn gas compositions to compare with changing weather and wind conditions. Duplicate samples from each probe position are reported for each day, but should not be considered gas samples of identical composition. Unfortunately, we cannot identify in all cases which of the duplicate samples was collected first. Though replicate analyses of the same gas are within precision reported in Appendix A, these duplicates demonstrate the variability of firn pore gas compositions that are possible with continued pumping. The drawdown time between first and second (or duplicate) sample is approximately 8-10 minutes or 16-20 liters of gas throughput. Figure 10 illustrates the comparison of CO_2 surface composition to station air temperature on a daily basis. The variation of carbon dioxide at "ground zero" with ambient air mass temperature is striking, especially the large spike of >2,300 ppmV CO_2 on August 9, which corresponds to a temperature warming to -7°C. Clearly, the ground boundary sublayer is not atmospheric in air gas composition. Release of carbon dioxide from the snow mass with warming conditions is indicated. This sublayer air mass does not rapidly mix with the bulk atmosphere on a calm windless day. Surface carbon dioxide otherwise is approximately 868 ppmV with a range of 755 to 2,318 ppmV.

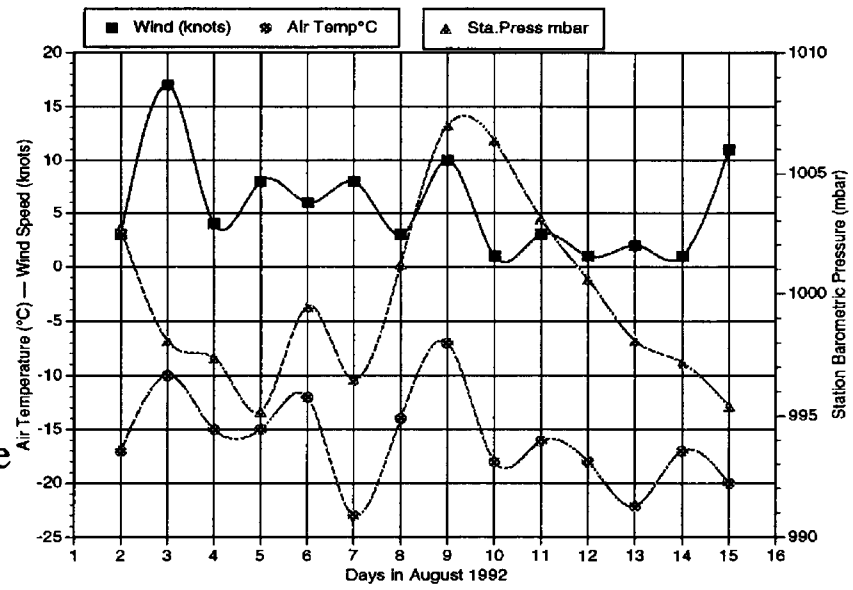

Figure 7. Comparison of wind speed, surface temperature, and station barometric pressure during firn gas sampling at GISP2.

At the 3.0 meter depth (fig. 11) carbon dioxide still shows a correlation with air temperature with an average CO_2 of 869 ppmV and a range of 681 to 926 ppmV. The CO_2 difference between first and second sample varies between several ppmV and >150 ppmV. CO_2 compositions of firn pore gases at 14.5 meters depth varied over the 13 day collection interval

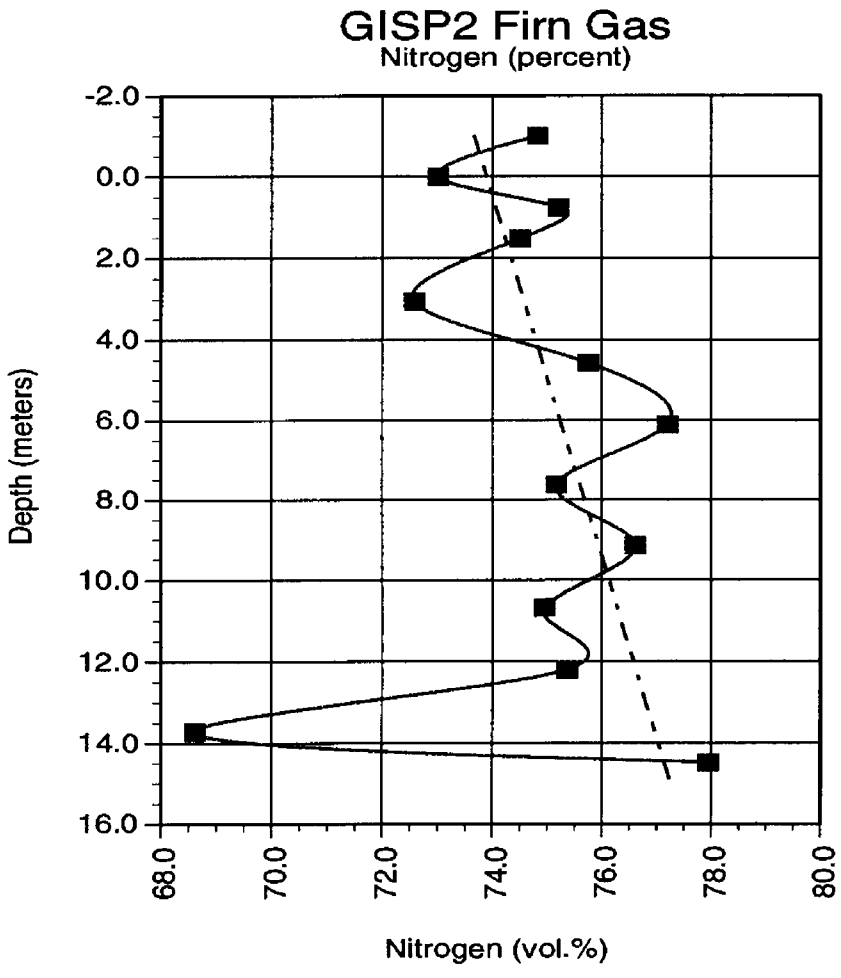

Figure 8a. Depth profile for nitrogen in firn to 14.5 meters, GISP2 Greenland.

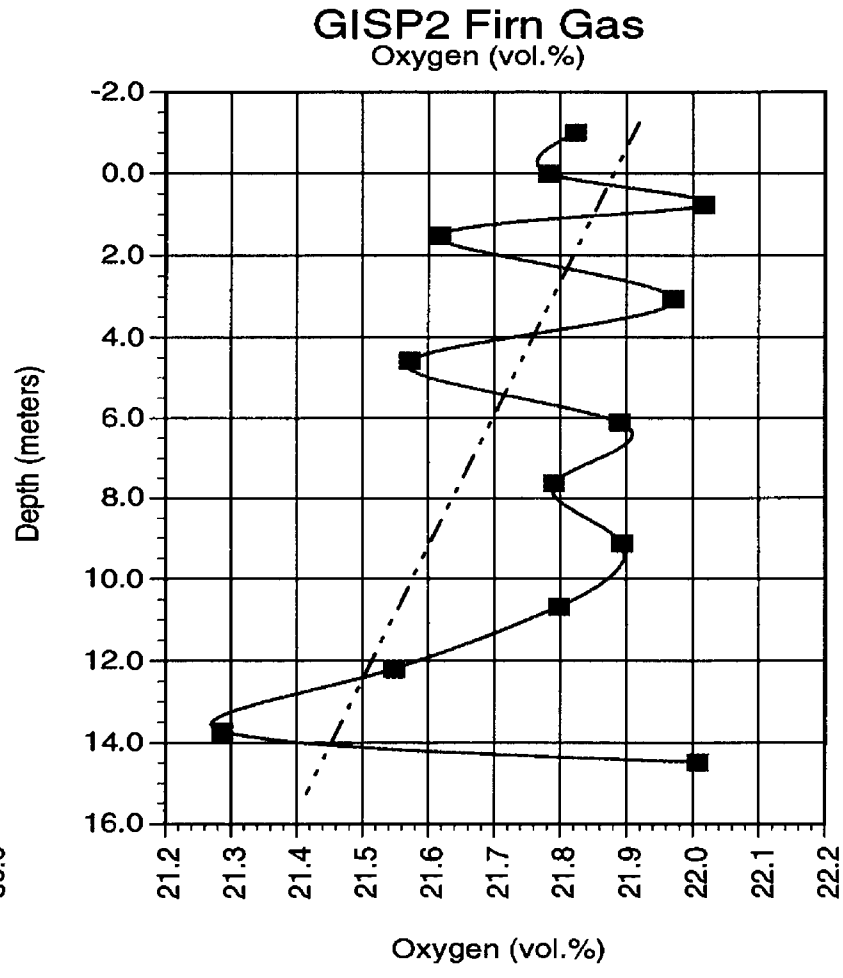

Figure 8b. Depth profile for oxygen in firn to 14.5 meters, GISP2 Greenland.

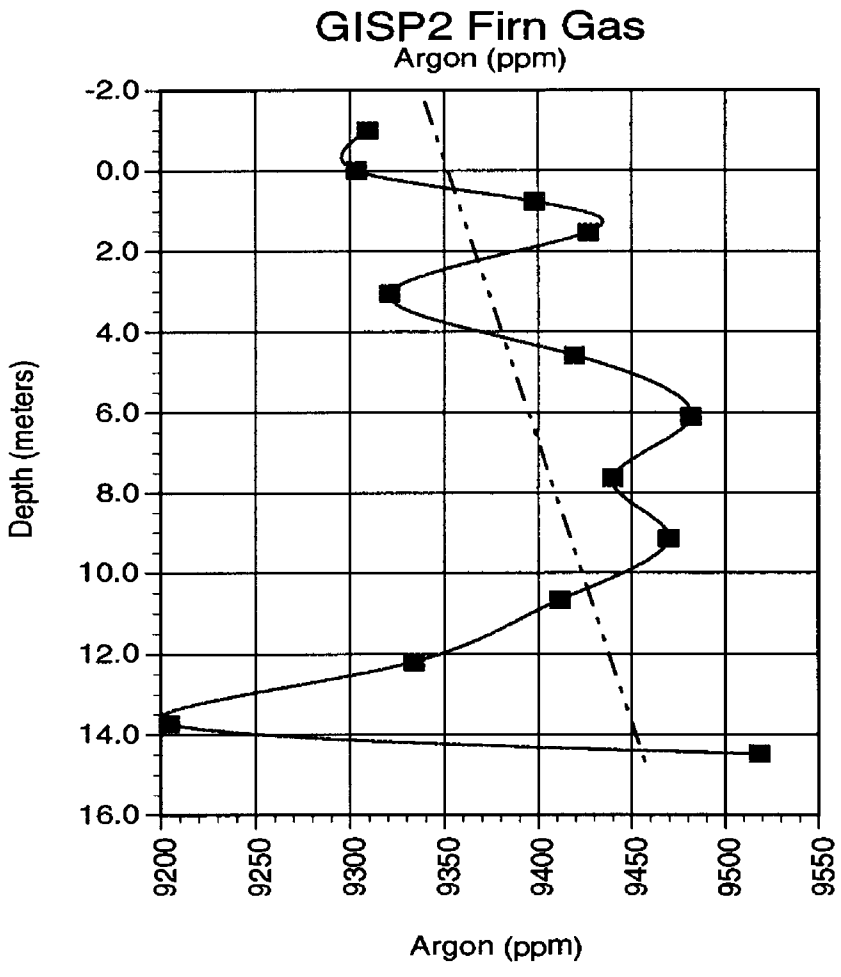

Figure 8c. Depth profile for argon in firn to 14.5 meters, GISP2 Greenland.

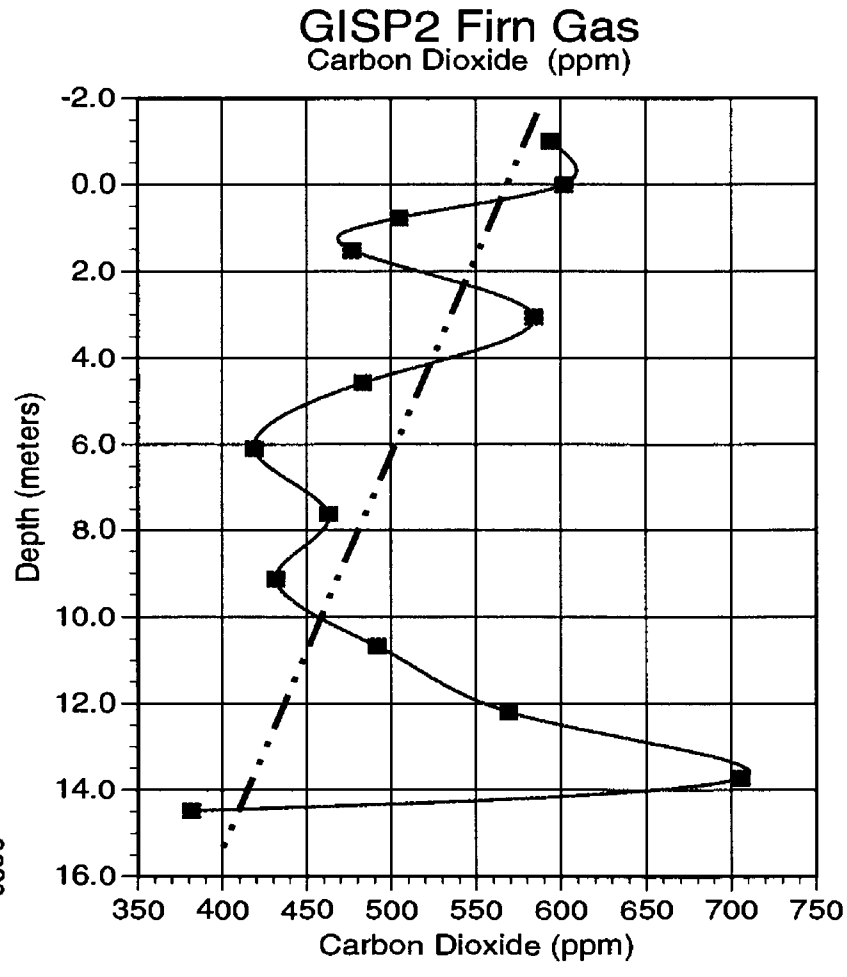

Figure 8d. Depth profile for carbon dioxide in firn to 14.5 meters, GISP2 Greenland.

between 751 and 1,311 ppmV with an average of 887 ppmV (fig. 12). The duplicate samples at this depth generally show a smaller spread in carbon dioxide values than the 3.0 meter depth suite.

Table 9 sorts the duplicate samples to select the "best" guess of which sample was taken first based upon field notes and position of the vial in the sample case. This sorting produced the columns of "select" values for the time series at both depths. These select data are compared to a computed average of the two analyses in the table and plotted in figure 13 with surface CO_2 compositions previously shown to vary in response to temperature. These firn gas data clearly indicate a response to warming from an average temperature of –17°C to –7°C, producing a large "ground zero" carbon dioxide concentration spike. This CO_2 spike propagates to depth by warming of the firn column and mixing of elevated surface CO_2 with firn gas in the pores. Propagation of this disturbance appears to reach the 3.0 meter depth by the next day, and the 14.5 meter depth some time later. A temperature drop to –22°C on August 13, after two days of dense fog, decreased the surface and firn depth carbon

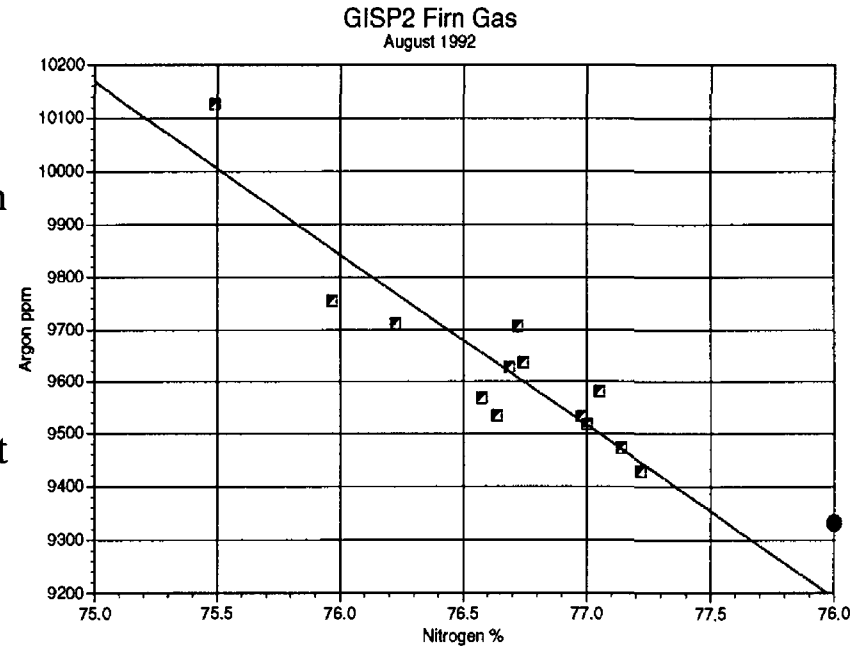

Figure 9a. GISP2 depth profile—argon vs. nitrogen.

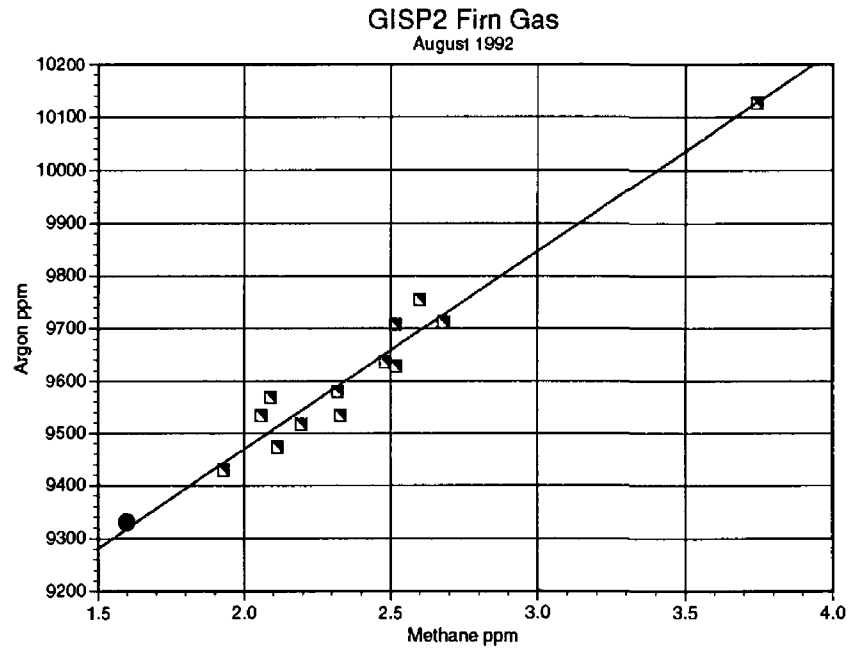

Figure 9b. GISP2 depth profile—argon vs. methane.

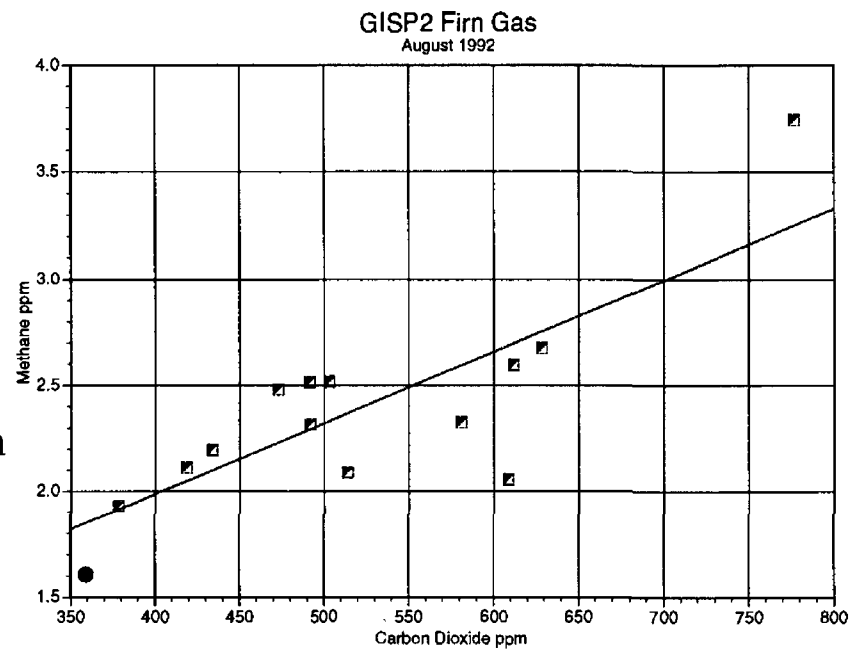

Figure 9c. GISP2 depth profile—methane vs. carbon dioxide.

Table 6. GISP2 firn gas time series sampling: surface, August 7 through August 15, 1992.

Date	Sample	Air Temp °C	Nitrogen %	N_2 ± σ	Oxygen %	O_2 ± σ	Argon ppm	Ar ± σ	CO_2 ppm	CO_2 ± σ
8/7/92	17 s	- 23.0	78.2468	0.0159	20.7622	0.0146	9083.4	14.4	827.19	0.60
8/8/92	18 s	- 14.0	78.1813	0.0130	20.8250	0.0116	9087.7	14.4	849.26	0.92
8/9/92	19 s	- 7.0	74.8025	0.0085	23.9554	0.0092	10102.0	14.6	2318.60	1.35
8/10/92	20 s	- 18.0	77.9079	0.0084	21.0662	0.0075	9447.0	13.2	811.61	0.37
8/11/92	21 s	- 16.1	77.9057	0.0165	21.0772	0.0138	9258.4	27.5	912.35	1.54
8/12/92	22 s	- 18.0	77.8566	0.0049	21.0995	0.0053	9523.7	15.1	915.84	0.91
8/13/92	23 s	- 22.1	78.1467	0.0272	20.8556	0.0259	9221.3	14.4	755.44	1.20
8/14/92	24 s	- 17.0	77.8247	0.0059	21.1501	0.0056	9356.9	5.9	895.50	2.07
8/15/92	25 s	- 20.0	77.8198	0.0120	21.1493	0.0113	9330.2	9.3	978.62	2.25

Table 7. GISP2 firn gas time series sampling: 3.0 meter depth, August 3 through August 15, 1992.

Date	Sample	Air Temp °C	Nitrogen %	N_2 ± σ	Oxygen %	O_2 ± σ	Argon ppm	Ar ± σ	CO_2 ppm	CO_2 ± σ
First										
8/3/92	13 b	- 10.0	78.1180	0.0081	20.8758	0.0076	9217.4	5.9	844.00	0.89
8/4/92	14 b	- 15.0	77.9593	0.0040	21.0304	0.0039	9212.9	4.8	890.40	1.02
8/5/92	15 b1	- 15.0	77.7952	0.0066	21.1745	0.0066	9438.2	4.4	865.05	0.80
8/6/92	16 b1	- 12.0	77.7494	0.0058	21.2222	0.0056	9456.5	5.1	827.54	0.95
8/8/92	18 b1	- 14.0	78.1657	0.0053	20.8356	0.0041	9196.7	15.0	790.29	0.55
8/9/92	19 b1	- 7.0	78.1192	0.0096	20.8807	0.0081	9193.3	23.8	807.46	0.62
8/10/92	20 b1	- 18.0	78.0845	0.0064	20.9291	0.0066	9119.8	19.7	744.25	0.51
8/11/92	21 b1	- 16.1	78.0320	0.0058	20.9821	0.0058	9108.4	19.8	750.32	0.42
8/12/92	22 b1	- 18.0	77.7750	0.0066	21.1831	0.0048	9628.3	19.3	791.08	0.68
8/13/92	23 b1	- 22.1	78.2001	0.0108	20.8037	0.0109	9280.8	4.9	681.13	1.95
8/14/92	24 b1	- 17.0	77.8956	0.0108	21.0798	0.0101	9337.8	10.4	908.54	2.15
8/15/92	25 b1	- 20.0	77.9469	0.0037	21.0318	0.0034	9287.8	4.5	925.75	1.98
Second										
8/5/92	15 b2	- 15.0	77.7278	0.0066	21.2420	0.0063	9467.8	5.0	834.36	0.86
8/6/92	16 b2	- 12.0	77.7140	0.0068	21.2595	0.0065	9471.2	5.8	793.89	0.72
8/7/92	17 b2	- 23.0	78.1175	0.0108	20.8742	0.0963	9211.6	13.5	871.36	0.83
8/8/92	18 b2	- 14.0	78.1730	0.0108	20.8214	0.0093	9211.7	15.8	843.49	0.62
8/9/92	19 b2	- 7.0	78.0359	0.0149	20.9681	0.0131	9197.4	20.1	763.32	0.55
8/10/92	20 b2	- 18.0	78.1576	0.0094	20.8494	0.0083	9029.6	16.7	900.44	0.47
8/11/92	21 b2	- 16.1	77.6277	0.0063	21.3576	0.0053	9266.1	18.1	881.16	0.75
8/12/92	22 b2	- 18.0	77.7999	0.0092	21.1517	0.0077	9584.7	16.5	899.20	0.50
8/13/92	23 b2	- 22.1	78.1756	0.0106	20.8291	0.0107	9264.5	5.5	688.93	1.84
8/14/92	24 b2	- 17.0	77.8799	0.0101	21.1041	0.0096	9342.4	8.2	817.78	2.54
8/15/92	25 b2	- 20.0	78.0418	0.0065	20.9400	0.0060	9266.5	5.1	915.40	2.47

dioxide values several hundred ppmV. A rapid recovery to previous elevated values is seen on August 14 and 15 with clearing skies, warming, and heavy hoar development and assisted by wind pumping. An increase in wind speed to approximately 11 knots from the previous days of 1-2 knots enhanced mixing and release of carbon dioxide. This time series variation in gas composition in response to documented weather conditions suggests important atmospheric gas transfer processes operating in the firn column (to be evaluated in the discussion to follow).

A detailed pumpdown experiment on August 12 from the 14.5 meter probe, after completion

Table 8. GISP2 firn gas time series sampling: 14.5 meter depth, August 3 through August 15, 1992.

Date	Sample	Air Temp °C	Nitrogen %	N_2 ± σ	Oxygen %	O_2 ± σ	Argon ppm	Ar ± σ	CO_2 ppm	CO_2 ± σ
First										
8/3/92	13 a	- 10.0	78.0600	0.0095	20.9317	0.0086	9257.4	11.4	825.65	0.93
8/4/92	14 a	- 15.0	77.2826	0.0078	21.6296	0.0072	9567.4	8.9	1311.10	1.09
8/5/92	15 a1	- 15.0	77.8629	0.0060	21.1094	0.0060	9435.1	3.9	842.18	1.31
8/6/92	16 a1	- 12.0	77.7320	0.0063	21.2364	0.0059	9460.0	6.6	855.90	1.07
8/7/92	17 a1	- 23.0	77.9098	0.0137	21.0644	0.0121	9259.6	15.6	998.49	0.73
8/8/92	18 a1	- 14.0	78.0347	0.0149	20.9673	0.0136	9196.4	14.0	783.66	0.61
8/9/92	19 a1	- 7.0	77.9239	0.0084	21.0541	0.0074	9254.7	11.7	965.83	0.99
8/10/92	20 a1	- 18.0	78.2621	0.0108	20.7648	0.0090	8910.1	21.8	820.72	1.05
8/11/92	21 a1	- 16.1	78.0434	0.0135	20.9662	0.0127	9129.3	16.4	774.85	0.61
8/12/92	22 a1	- 18.0	77.7780	0.0073	21.1781	0.0055	9580.3	21.7	858.93	0.61
8/13/92	23 a1	- 22.1	78.0409	0.0081	20.9407	0.0082	9421.1	7.6	763.15	1.65
8/14/92	24 a1	- 17.0	77.8475	0.0085	21.1216	0.0082	9353.4	5.1	956.08	2.67
8/15/92	25 a1	- 20.0	77.8905	0.0041	21.0842	0.0040	9311.9	4.9	940.83	2.48
Second										
8/5/92	15 a2	- 15.0	77.7632	0.0051	21.2039	0.0049	9443.6	4.2	885.19	0.45
8/6/92	16 a2	- 12.0	77.5956	0.0051	21.3766	0.0046	9556.6	6.9	823.59	0.65
8/7/92	17 a2	- 23.0	78.2638	0.0140	20.7408	0.0128	9089.6	12.1	864.76	0.55
8/8/92	18 a2	- 14.0	78.0929	0.0204	20.9057	0.0185	9205.2	18.5	808.45	0.52
8/9/92	19 a2	- 7.0	77.9375	0.0080	21.0591	0.0074	9194.1	11.7	839.91	0.58
8/10/92	20 a2	- 18.0	78.1827	0.0088	20.8385	0.0075	9031.1	19.7	756.10	0.35
8/11/92	21 a2	- 16.1	78.2057	0.0110	20.8100	0.0099	9018.5	15.0	824.79	0.45
8/12/92	22 a2	- 18.0	77.8450	0.0104	21.1155	0.0089	9569.8	16.8	825.56	0.46
8/13/92	23 a2	- 22.1	78.1078	0.0142	20.8878	0.0141	9293.7	6.1	751.00	2.30
8/14/92	24 a2	- 17.0	77.8002	0.0310	21.1811	0.0293	9382.7	17.3	803.86	1.80
8/15/92	25 a2	- 20.0	77.8604	0.0052	21.1077	0.0051	9332.5	5.1	986.91	2.57

Table 9. GISP2 Firn gas data: analysis of repeat samples.

Date	Air Temp °C	Surface	3.0m	3.0m duplicate	3.0m avg.	3.0m Select	14.5m	14.5m duplicate	14.5m avg.	14.5m Select
8/2/92	-17.0		675.29		675.29	675.29	577.19		577.19	577.19
8/3/92	-10.0		844.00		844.00	844.00	825.65		825.65	825.65
8/4/92	-15.0		890.40		890.40	890.40	1311.10		1311.10	
8/5/92	-15.0		865.05	834.36	849.71	865.05	842.18	885.19	863.69	842.18
8/6/92	-12.0		827.54	793.89	810.72	827.54	855.90	823.59	839.75	823.59
8/7/92	-23.0	827.19		871.36	871.36	871.36	998.49	864.76	931.63	864.76
8/8/92	-14.0	849.26	790.29	843.49	816.89	843.49	783.66	808.45	796.06	808.45
8/9/92	-7.0	2318.60	807.46	763.32	785.39	807.46	965.83	839.91	902.87	839.91
8/10/92	-18.0	811.61	744.25	900.44	822.35	900.44	820.72	756.10	788.41	820.72
8/11/92	-16.1	912.35	750.32	881.16	815.74	881.16	774.85	824.79	799.82	824.79
8/12/92	-18.0	915.84	791.08	899.20	845.14	899.20	858.93	825.56	842.25	858.93
8/13/92	-22.1	755.44	681.13	688.93	685.03	688.93	763.15	751.00	757.08	751.00
8/14/92	-17.0	895.50	908.54	817.78	863.16	817.78	956.08	803.86	879.97	803.86
8/15/92	-20.0	978.62	925.75	915.40	920.58	915.40	940.83	986.91	963.87	940.83

Table 10. GISP2 Firn gas pumpdown series sampling: 14.5 meter depth, August 12, 1992.

Sample	Pump Interval seconds	Cumulative Time seconds	Nitrogen %	N_2 ± σ	Oxygen %	O_2 ± σ	Argon ppm	Ar ± σ	CO_2 ppm	CO_2 ± σ
PS-1	0	0	77.8267	0.0123	21.1314	0.0110	9543.9	14.5	875.27	0.48
PS-2	10	10	77.7066	0.0115	21.2442	0.0100	9599.1	16.6	892.60	0.40
PS-3	10	20	77.6862	0.0116	21.2793	0.0102	9606.5	14.5	738.53	0.60
PS-4	10	30	77.7096	0.0132	21.2442	0.0114	9576.2	18.6	885.76	0.85
PS-5	15	45	77.7029	0.0080	21.2496	0.0094	9544.5	21.0	930.18	0.64
PS-6	15	60	77.7321	0.0064	21.2325	0.0078	9460.7	29.5	892.39	0.99
PS-7	30	90	77.7864	0.0147	21.1682	0.0128	9388.0	28.5	1065.90	2.29
PS-8	30	120	77.7656	0.0179	21.2070	0.0149	9315.8	32.4	957.60	2.55
PS-9	30	150	77.6052	0.0072	21.3418	0.0084	9567.3	32.3	962.27	0.90
PS-10	30	180	77.7152	0.0157	21.2315	0.0135	9555.1	23.7	977.56	0.66
PS-11	30	210	78.2815	0.0201	20.7078	0.0168	9275.4	33.0	831.18	1.39
PS-12	30	240	78.1265	0.0142	20.8805	0.0131	9127.3	16.1	802.87	1.12
PS-13	30	270	78.0494	0.0070	20.9473	0.0083	9203.7	22.3	829.31	0.46
PS-14	30	300	78.0393	0.0066	20.9583	0.0068	9201.4	23.1	822.77	0.47
PS-15	60	360	78.0574	0.0070	20.9395	0.0085	9185.7	21.2	845.10	0.81
PS-16	60	420	78.0782	0.0159	20.9086	0.0130	9254.5	29.5	876.85	1.43
PS-17	60	480	77.9345	0.0215	21.0497	0.0184	9319.1	31.4	838.92	1.61
PS-18	60	540	77.8315	0.0480	21.1341	0.0441	9439.2	36.7	905.27	2.10
PS-19	60	600	77.9905	0.0117	20.9868	0.0097	9298.2	34.2	929.64	1.78

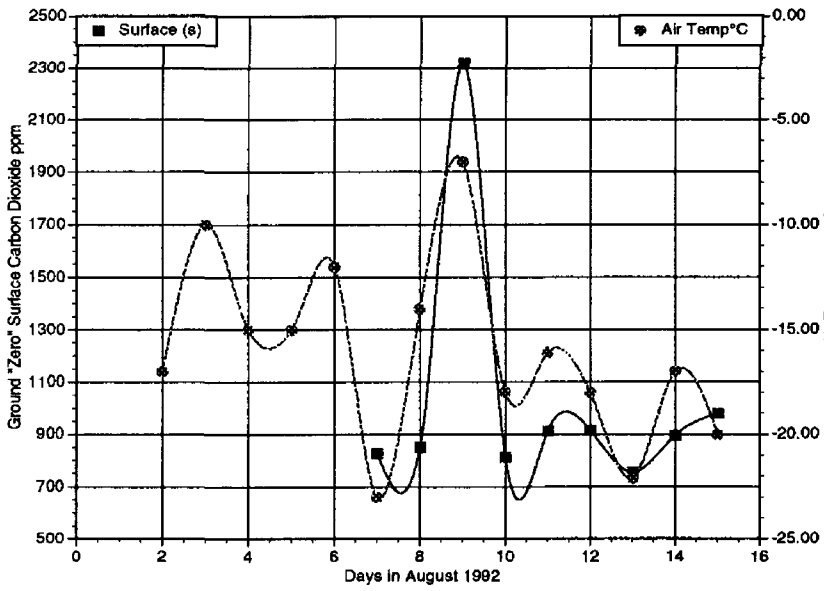

Figure 10. Variations in "ground zero" surface CO_2 and temperature, GISP2, Greenland.

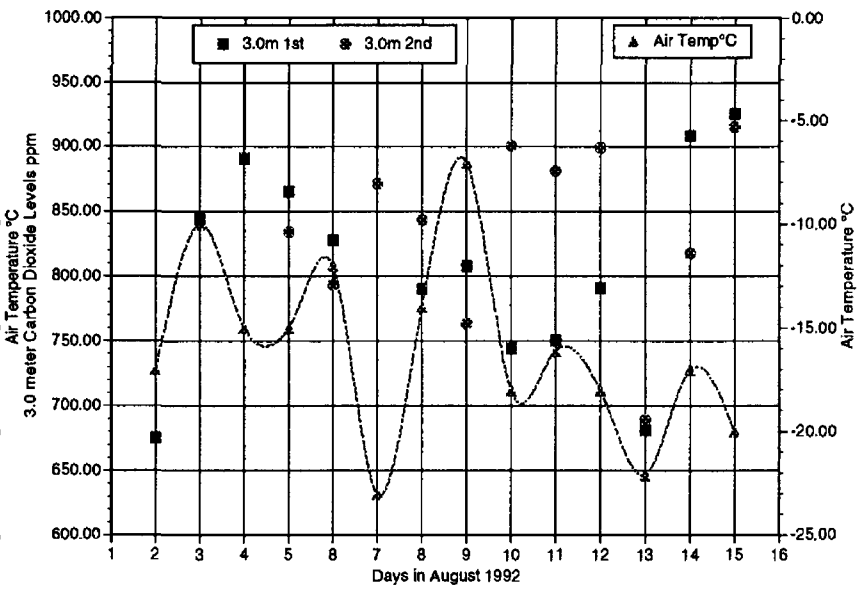

Figure 11. Variations in 3.0 meter deep CO_2, GISP2, Greenland.

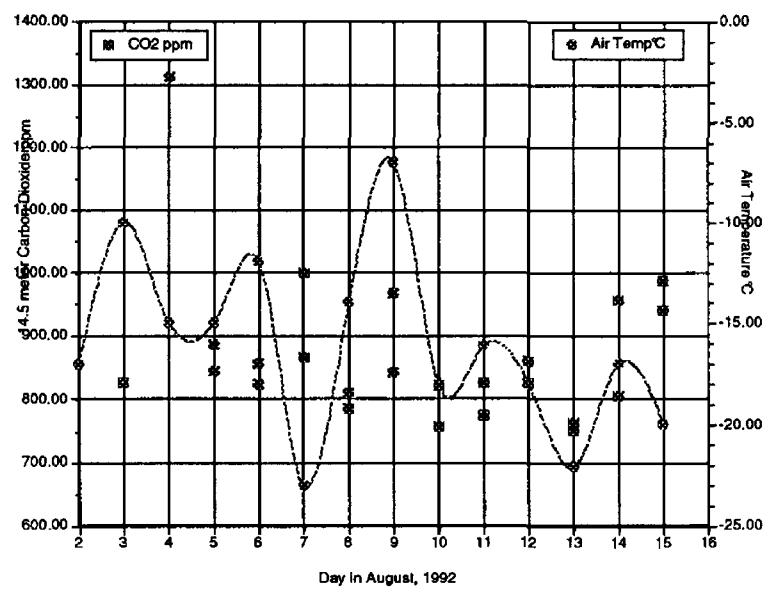

Figure 12. Variations in 14.5 meter deep CO_2, GISP2, Greenland.

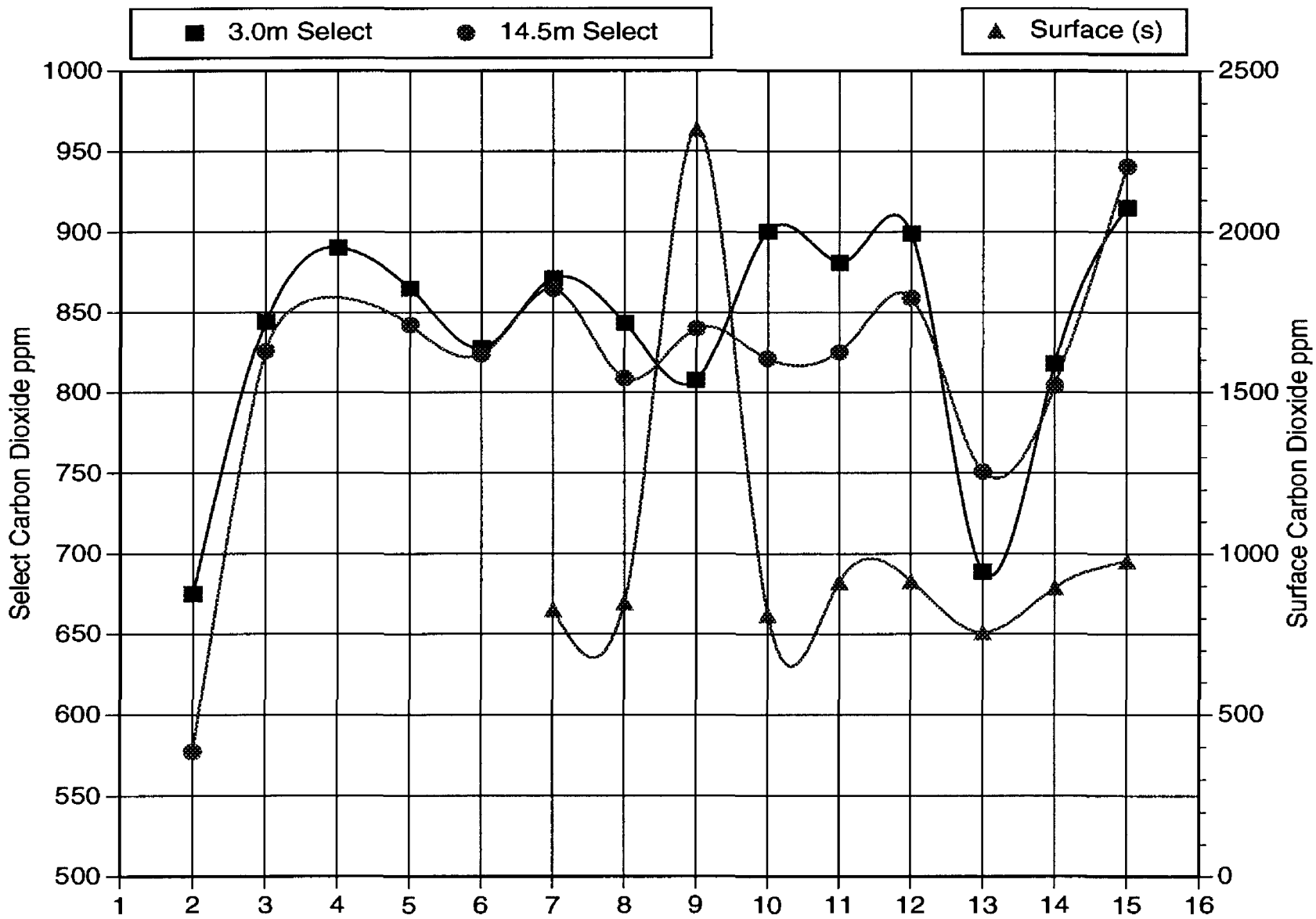

Figure 13. Variations in CO_2 showing time-space dependency resolved on a 24-hour sampling interval from the surface, 3.0 meters, and 14.5 meters depth in firn. Warming event on August 9 (-7°C) created a CO_2 spike at the surface of >2,300 ppmV which is propagated to 3.0 meters by the next day, and to 14.5 meters 1-2 days later. Other parallel changes reflect similar time lags with depth and show a response to variable cloud cover, fog, wind conditions, and temperature changes. GISP2, Greenland.

of the daily time series sampling, yielded 19 consecutive samples (table 10) over a total drawdown pumping interval of 10 minutes (20 liters). Sampling required a total elapsed time of about 1 hour 20 minutes, and was preceded by 8-10 minutes of pumping for the daily time series samples. Analyses are plotted against pumpdown time (seconds) with one sigma error bars in figure 14 a-d. Two drawdown intervals are indicated in these plots. The first 3-4 minutes of pumping sampled pore volumes of variable amounts of stagnant air-like gas and anomalous firn gas. Continued pumping produced a drawdown gas further from the probe tip with compositions varying systematically. This second (continued) pumpdown interval suggests a chromatographic separation of gases in the snowpack and an overall enrichment of carbon

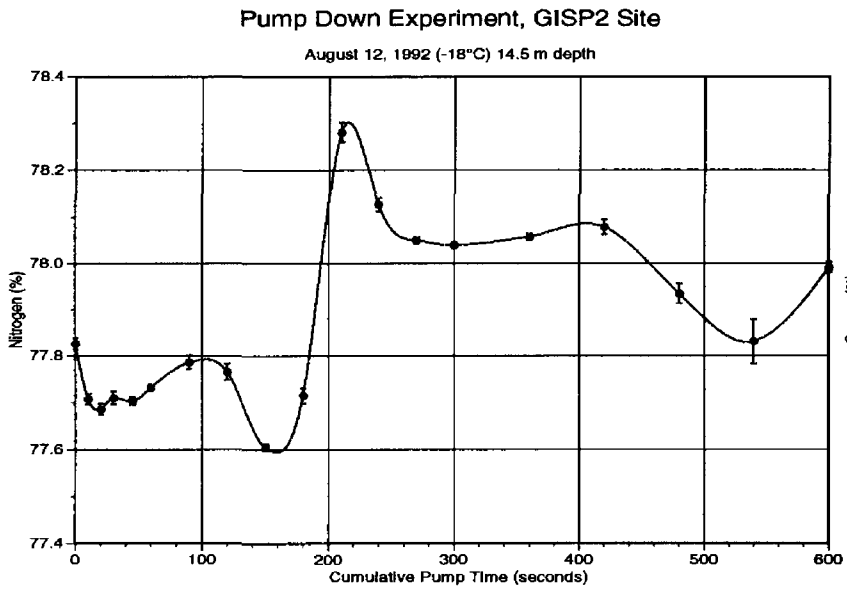

Figure 14a. Pumpdown experiment. Nitrogen change with continued pumping for 10 minutes. GISP2.

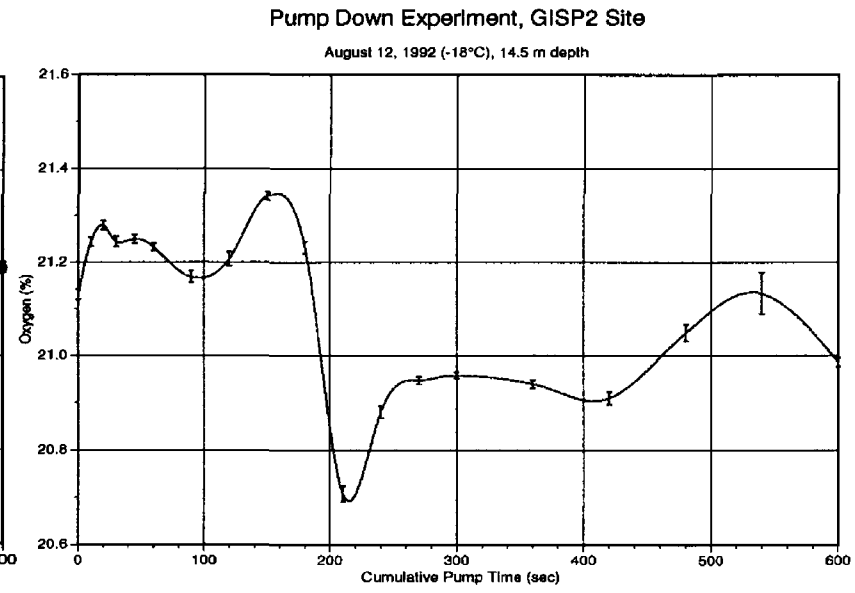

Figure 14b. Pumpdown experiment. Oxygen change with continued pumping for 10 minutes. GISP2.

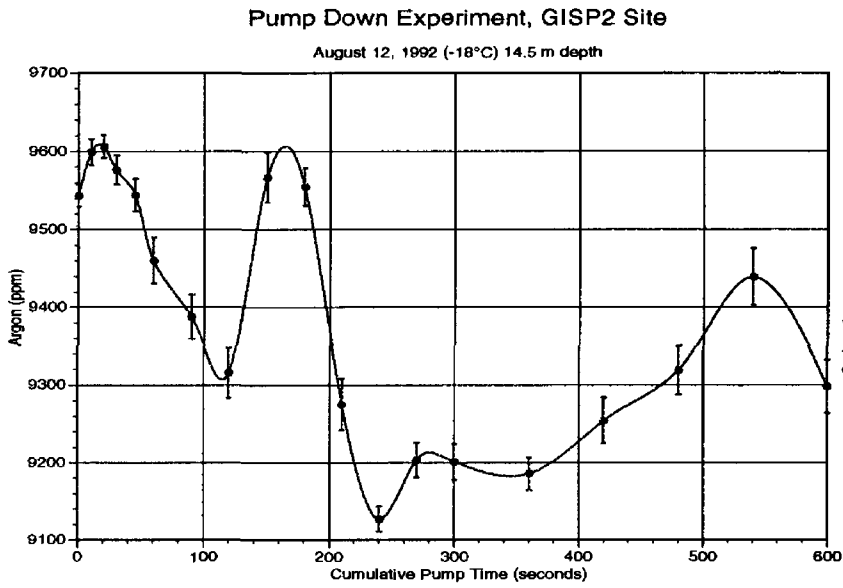

Figure 14c. Pumpdown experiment. Argon change with continued pumping for 10 minutes. GISP2.

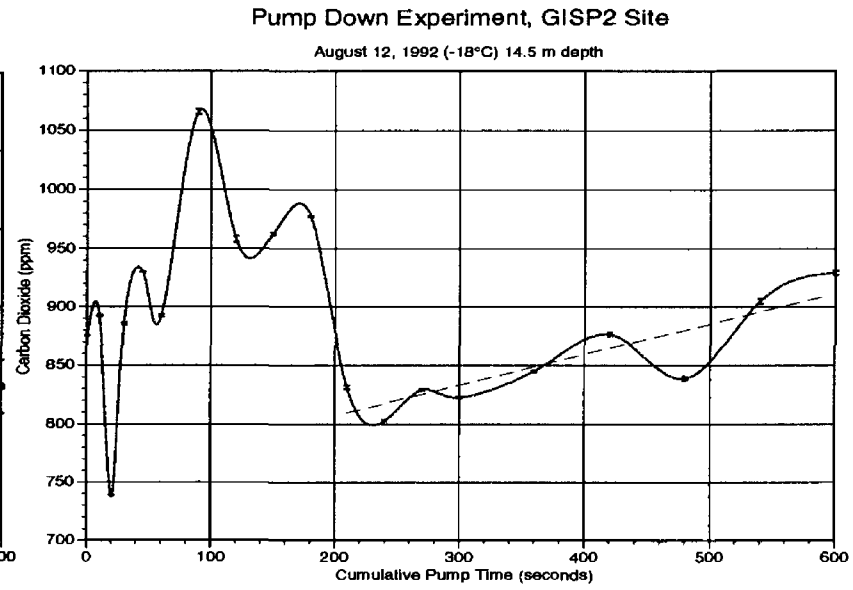

Figure 14d. Pumpdown experiment. Carbon dioxide change with continued pumping for 10 minutes. GISP2.

dioxide with continued pumping.

Taylor Dome, Antarctica Study Area —In January 1993, two depth profiles were sampled near the Taylor Dome drill site (Grootes, Steig, and Massey, 1991; Waddington, Morse, and others, 1991). The northern probe was placed 300 meters from the intersection of the surveyed Center Line and 20 Line on a bearing 25° SSE. This probe penetrated to 4.5 meters and was sampled at four depths in a southerly 30 knot wind. The second probe was placed 10 meters to the south of the northern probe on a line perpendicular to the Center Line and penetrated to 10 meters. Eight depths were sampled under prevailing southerly 5 knot winds. These data are reported in table 11. The depth profile series are plotted in figure 15 a-d. Nitrogen and argon are depleted relative to atmosphere, whereas oxygen and, strikingly, carbon dioxide are enriched.

Table 11. Taylor Dome, Antarctica firn gas depth profile data.

a. Shallow North Sampling Probe (≈ 30 knot winds)

Sample	Depth meters	Nitrogen percent	N_2 $\pm\sigma_x$	Oxygen percent	O_2 $\pm\sigma_x$	Argon ppm	Ar $\pm\sigma_x$	Carbon Dioxide ppm	CO_2 $\pm\sigma_x$
mdd_0000	0.0	77.2674	0.0121	21.6888	0.0109	9329.6	9.24	1108.20	4.05
mdd_0015	1.5	77.5349	0.0045	21.4315	0.0042	9217.1	3.39	1118.60	3.05
mdd_0030	3.0	78.0645	0.0048	20.9530	0.0047	9173.3	3.73	651.71	2.31
mdd_0045	4.5	77.8824	0.0059	21.1263	0.0055	9155.5	3.85	757.94	2.52

b. Deep South Sampling Probe (≈ 5 knot winds)

Sample	Depth meters	Nitrogen percent	N_2 $\pm\sigma_x$	Oxygen percent	O_2 $\pm\sigma_x$	Argon ppm	Ar $\pm\sigma_x$	Carbon Dioxide ppm	CO_2 $\pm\sigma_x$
mdn_0000	0.0	77.0619	0.0116	21.8755	0.0102	9412.7	9.09	1212.90	5.57
mdn_0015	1.5	78.0442	0.0023	20.9514	0.0039	9235.6	4.48	808.37	2.17
mdn_0030	3.0	78.4706	0.0048	20.5458	0.0045	9183.8	3.77	652.48	1.20
mdn_0045	4.5	78.4448	0.0054	20.5711	0.0052	9208.4	3.01	631.88	2.26
mdn_0060	6.0	78.1973	0.0038	20.8005	0.0035	9239.8	4.72	782.25	1.67
mdn_0075	7.5	78.3597	0.0064	20.6512	0.0061	9207.8	3.93	682.90	2.04
mdn_0090	9.0	78.1705	0.0058	20.8342	0.0054	9243.5	6.60	709.71	1.90
mdn_0100	10.0	77.5199	0.0061	21.4071	0.0059	9571.4	4.46	1158.80	2.62

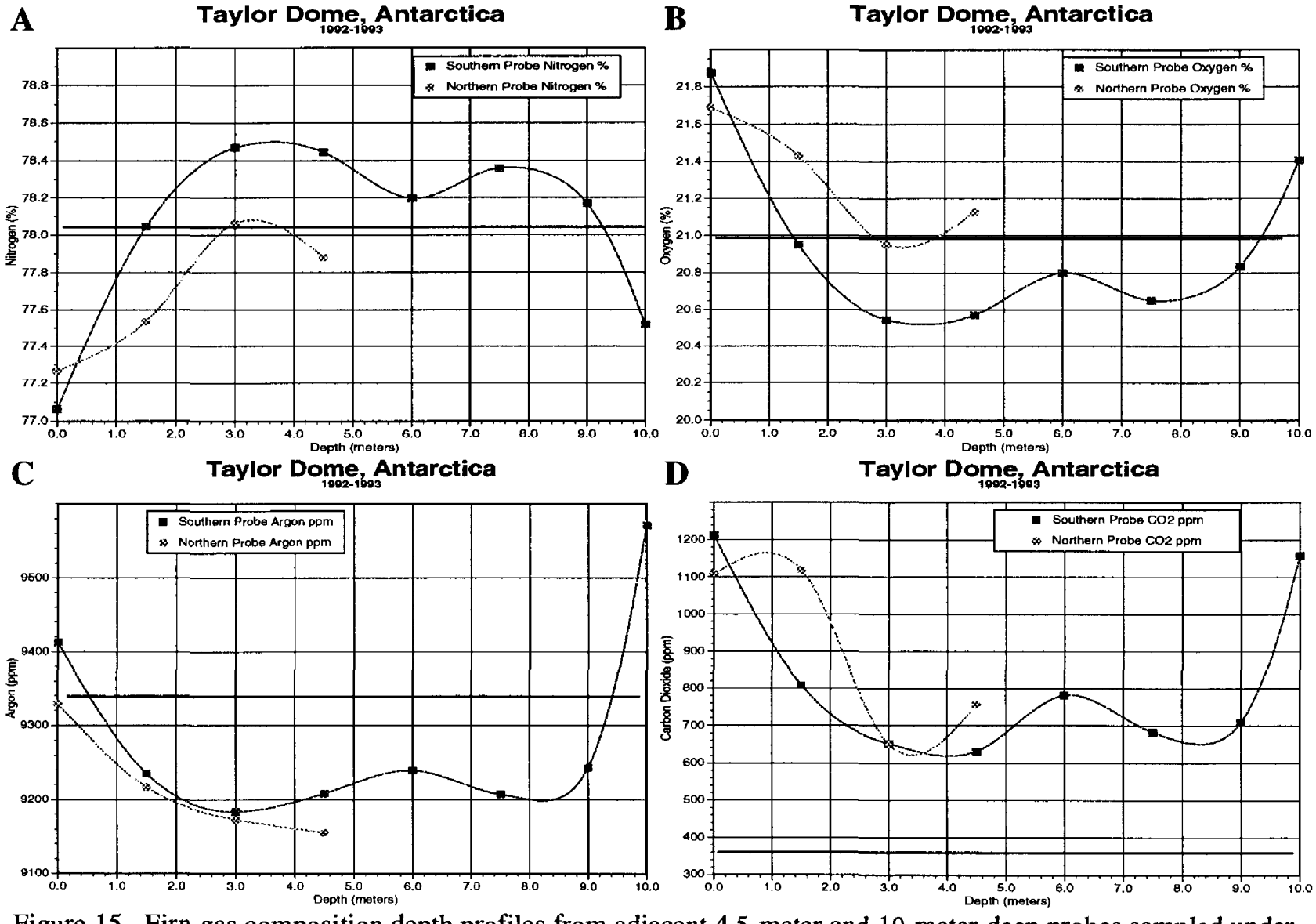

Figure 15. Firn gas composition depth profiles from adjacent 4.5-meter and 10-meter-deep probes sampled under near identical weather conditions with exception of wind speed as noted in text. Taylor Dome, Antarctica.

Compositional differences between the two probe sample profiles cannot be assigned to different firn conditions over a 10 meter distance. Compositional differences likely are a function of wind pumping and chromatographic effects related to the large difference in wind speed during the two sampling periods under otherwise near identical weather and firnification conditions. Nitrogen and argon are depleted and oxygen and carbon dioxide are enriched in samples collected during high wind conditions. With the exception of argon, these differences are the same as observed at GISP2 for the pumpdown experiment and are an indication of the effects expected with air movement through snowpack. Nitrogen versus carbon dioxide is plotted (fig. 16) to illustrate the inverse correlation between a major and a minor gas component in the samples.

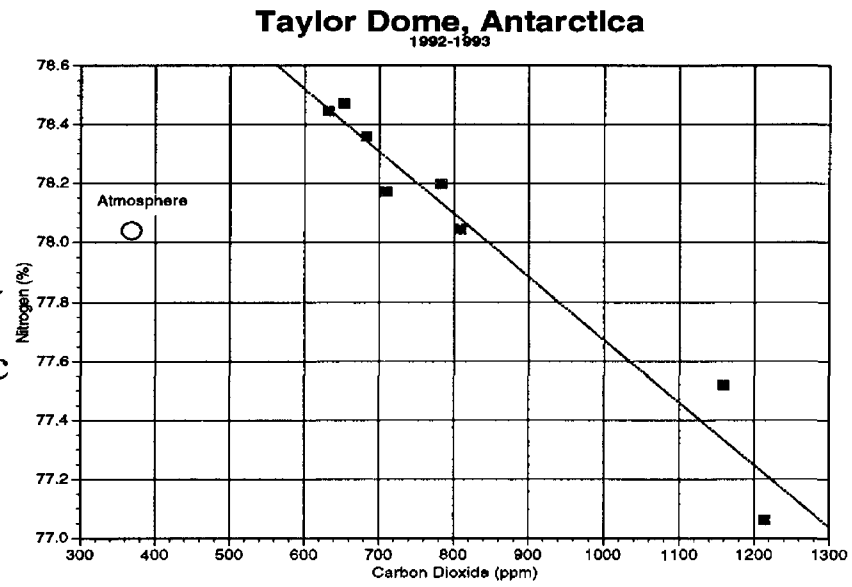

Figure 16. Inverse relationship of nitrogen (a major gas) with carbon dioxide (a trace gas) indicating variations in firn gas compositions are not a numerical artifact of analysis. Taylor Dome, Antarctica.

Discussion

Glacier ice contains a small amount of air entrapped as small bubbles during the transformation of snow to ice. Reconstruction of the composition of ancient atmosphere via analysis of the gas in these bubbles requires a precise understanding of the transfer processes whereby atmospheric gas has been isolated in gas bubbles. Important processes occur through the firn column that modify the atmospheric gas composition prior to closure of pores across the firn-ice transition. Our firn gas compositions are significantly different from modern atmosphere, are in contrast with published results of others (Bender, Sowers, and others, 1994; Schwander, Barnola, and others, 1993; Sowers, Bender, and Raynaud, 1989). Our data cannot be dismissed easily on the basis of sampling methods, sample containers, instrumentation, calibration, or standardization. We strongly argue from the time-space framework of the data, the consistent calibration and instrumental precision, and method of sampling, that these data

express the natural variations in firn pore gases. Other researchers have reported compositions similar to air because of their use of a much greater pumpdown time before sampling, and because of the complex and difficult problem of sampling small pore volume gases in a quasi-open system under conditions of extreme temperature contrast and the presence of both liquid and solid phases. The few published investigations describe methods not suited for sampling within the first several meters depth, or for conducting time series and pumpdown experiments as described in this report. Our results predict non-air-like gas would dominate firn pores only in the first few tens of meters, with effects dissipating at depth well before reaching closeoff at the firn-ice transition.

Prevailing local weather conditions and mechanisms of snow accumulation appear from our results to be important factors in determining shallow firn gas compositions. This point is illustrated by comparing the average carbon dioxide concentrations from 3200 meter elevation on the Klutlan Glacier, Alaska ($CO_{2\ avg.}$ = 1,922 ppmV; and $T_{mean\ annual}$ = –17°C) with that of the ascent samples ranging to 4,400 meters elevation ($CO_{2\ avg.}$ = 1,212 ppmV; and $T_{mean\ annual}$ = –24°C), and values from GISP2 in Greenland at 3,208 meters ($CO_{2\ avg.}$ = 878 ppmV; and $T_{mean\ annual}$ = –31°C), and Taylor Dome, Antarctica at 2,450 meters ($CO_{2\ avg.}$ = 710 ppmV; and $T_{mean\ annual}$ = –45°C). These data (fig. 17) demonstrate the importance of mean annual temperature (site weather conditions) on determining the shallow firn pore carbon dioxide. We note that similar elevated carbon dioxide levels are obtained from temperate regimes and Arctic snowpack sites (Coyne and Kelley, 1974; Sommerfeld, Musselman, and others, 1991), although these researchers ascribe elevated CO_2 in snowpack to biologic sources. Their reported values for carbon dioxide enrichment are 2x-6x atmospheric levels and, as reported, cannot all be attributed to biologic metabolism.

Conditions of net snow accumulation and prevailing weather range from sub-polar to temperate in Alaska, to polar conditions in Greenland, to extreme polar conditions in Antarctica. Carbon dioxide concentrations in near-surface firn voids are different for temperate (ice at pressure melting curve with presence of capillary liquid throughout firn column), cold

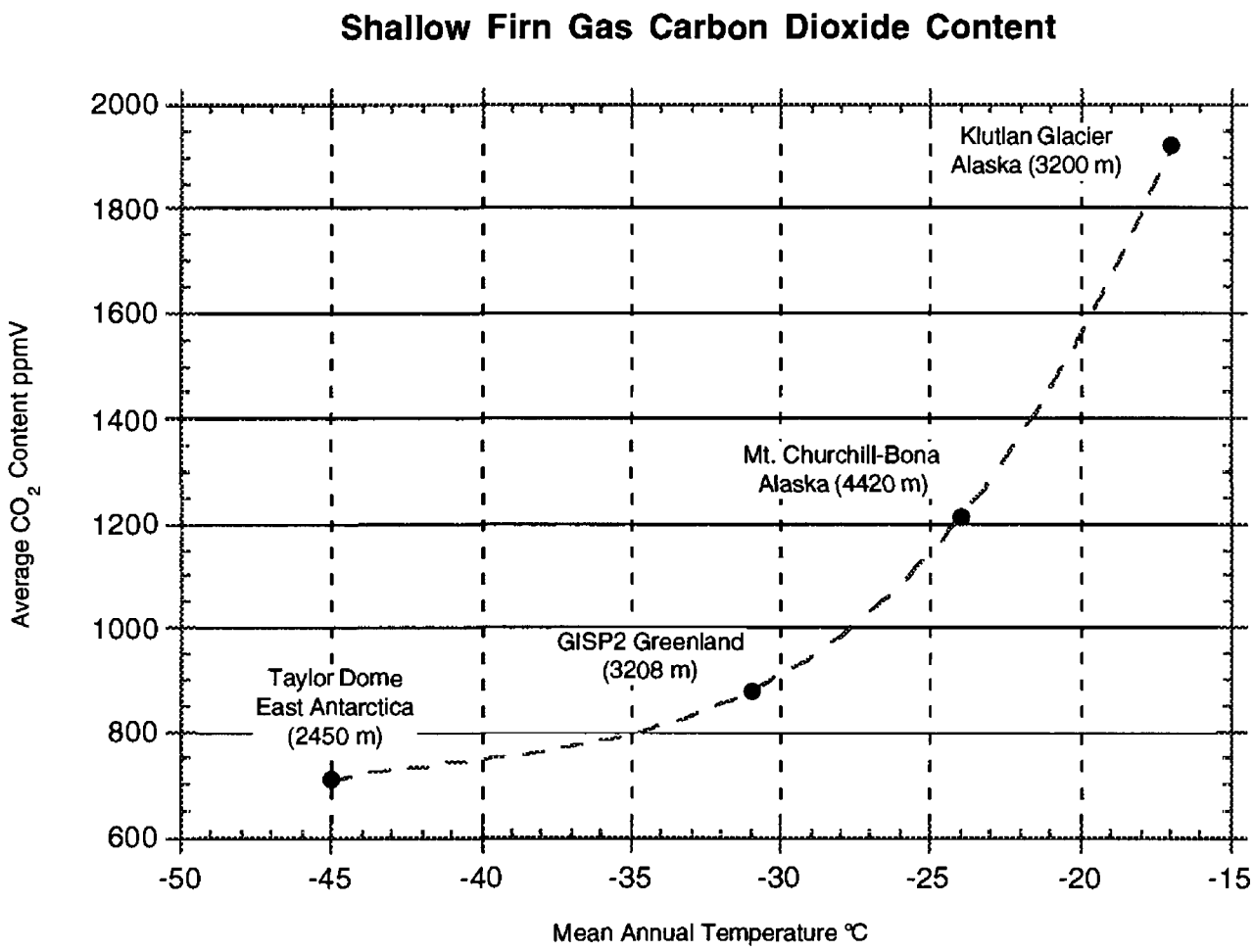

Figure 17. Dependence of average shallow firn gas carbon dioxide concentration on mean annual temperature of sites that range from sub-temperate, to polar, to extreme polar conditions of accumulation.

percolation zone (surface melting and hoar), and cold dry snow zone (no surface melting, extreme cold) glaciers. The compressed and sintered snow or firn undergoes diagenesis or metamorphism with compaction, deformation of ice grains, sublimation, melting, and recrystallization. With increasing depth, pore volumes and permeability decrease, density increases from ≈ 0.2 g/cc to > 0.8 g/cc, and ice grains increase in size with increased development of preferred orientation and stable interfacial grain boundaries. Densification is controlled mainly by mean temperature and accumulation rate. The rate of closure of pore volumes and the coarsening of ice grains dramatically affects the air transfer through firn and exchange with the ice. Because of different gas solubilities, the presence of a liquid melt phase, or even a thin liquid membrane film along grain boundaries, can have a major impact on determining the composition of gas ultimately isolated as bubbles in ice.

We propose an interpretation of our firn gas data that examines air sources, inputs and

losses to pore gases. Certainly gas in the intricate voids of shallow snow is subject to open exchange with the atmosphere via wind pumping and barometric pressure driven uptake and expulsion (Colbeck, 1989; Davidson, 1989; Martinerie, Lipenkov, and others, 1994; Schwander, 1989; Schwander, Barnola, and others, 1993). At greater depths in the firn column, molecular diffusion, gravitational stratification, and a general outward expulsion of gas with densification of the firn occurs (Craig, Horibe, and Sowers, 1988). These processes alone should produce air gas compositions similar to the atmosphere. The >2-3 times enrichment in carbon dioxide from atmosphere requires additional mechanism(s). We call upon selective wet deposition of gases onto snow to enrich CO_2. Dry deposition in the absence of precipitation does not have the selective adsorption potential to concentrate carbon dioxide (Davidson, 1989). Cloud air masses become supersaturated with respect to water, in large measure because of the increased ΔP_{vapor} associated with very small water droplet aerosols and surface effects. For a 0.01μm radius water droplet, the vapor pressure difference across the liquid-vapor interface is positive and approximately 1.114 from the Young and Laplace and the Kelvin equations (Adamson, 1982). This increase in vapor pressure increases the solubility of carbon dioxide in water beyond its already more than 72x greater solubility than nitrogen (Wilhelm, Rattino, and Wilcock, 1977). [Note that at 273.15°K and 1 atm the Ostwald coefficients, defined as the ratio of volume of pure gas absorbed by volume of water, are N_2 = 0.02381, O_2 = 0.04902, Ar = 0.05360, CO_2 = 1.717, CH_4 = 0.05729, N_2O = 1.286.] With rapid nucleation and snow crystallization (with or without an evaporation or condensation step), strong in-cloud scavenging of carbon dioxide should occur on ice nuclei that would produce snow fallout strongly enriched in carbon dioxide. Non-hygroscopic sorption of gases onto forming ice crystals additionally would enrich gases selectively by both physico- and chemsorption on large, highly activated sorption surface areas. Small gas bubbles can form in ice crystals but normally at no more than approximately 1 percent of total trapped air (Schwander, 1989). With riming and in-cloud scavenging, large volumes of gas can be delivered to the accumulating snowfall that will be strongly CO_2 enriched. Post-accumulation snow surfaces may affect

additional air gas dry deposition in other than extremely cold polar conditions by absorption, diffusion, and solution. These latter processes are presumed to have a small effect in concentrating carbon dioxide because rapid diagenesis of snow would tend to release gas, not retain it. Subsurface summer hoar layers will release much of this sorbed gas in non-atmospheric concentrations during sublimation and coarsening recrystallization of ice. With continued recrystallization and coarsening of the firn, a flux of CO_2-enriched air is released to the pore spaces. A first order approximation to this flux intensity would parallel a $\Delta\rho$ (rate of density change) profile with depth. The process is accelerated with warming to create a net flux of carbon dioxide to the snow surface "ground zero" boundary sublayer atmosphere (as observed at GISP2 on August 9 when CO_2 reached 2,300 ppmV during warming to –7°C).

Shallow firn gas compositions then are seen to be the balance of fluxes into and out of the firn pore volumes. Shallow pore volume gas input is dominated by desorption fluxes and to a lesser extent, a transfer of atmospheric gases through the pores by wind pumping and barometric pressure changes. The desorption gas flux exponentially diminishes to a depth (15-20 meters) where throughput of atmospheric gases from the surface becomes the main control on pore gas composition. Prolonged calm, stable (and especially warm) weather seasonally can create a surface boundary sublayer air composition unlike the homogenized atmosphere above by diffusional loss from the firn of desorption gases. More intense weather can produce a well-mixed atmosphere virtually destroying the boundary sublayer. As such, we suspect the depth to which desorption fluxes dominate firn pore gas chemistry largely depends upon prevailing and seasonal local weather. Overprinted upon the dynamics of shallow firn gas chemistry is the minor net outward loss of gas from densification of the firn column. This throughput flux should be similar to deeper more air-like firn gas, with minor modifications from chromatographic and diffusional effects.

Below the level of flux crossover in the firn column the continued throughput of air dominates. Major interconnected pore volumes that define the net permeability will continue to exchange with air. Smaller volumes that are less well interconnected may continue to receive a

major flux of sorption gases and exhibit non-atmosphere air compositions. Based upon ^{14}C measurements (Alex Wilson; oral commun., 1995), nearly 25 percent excess carbon dioxide is present in the ice matrix that has not experienced seasonal hoar sublimation loss and recrystallization. We suggest that this matrix gas is our anomalous shallow firn gas not completely purged during diagenesis and still retained in micropore volumes, crystal boundary and junction voids, and in crystal defects. Perhaps very little of this "matrix" gas ultimately is incorporated into major gas bubbles in ice, but it is readily detected in the compositional contrast between wet and dry extraction methods. This matrix component would be critical to determining gas chemistry from deeper coarsened ice, especially below the enclathratization depth. Decompression of extracted ice cores and re-nucleation of gas bubbles from clathrates possibly will incorporate this matrix gas in the re-formed bubbles along with the air gases.

Conclusion

Our firn gas chemistry data are in striking contrast to expected and assumed values. Results suggest complex processes starting with possible in-cloud scavenging and wet deposition of air gases in non-atmospheric concentration levels. Shallow firn gas compositions are controlled by desorption gas fluxes and are extremely (2x-3x atmosphere) enriched in CO_2. At moderate depths in the firn column, net permeability and larger interconnected pore volumes continue to exchange gases with the atmosphere and control the composition of gas ultimately sealed in gas bubbles at closure across the firn-ice transition. Anomalous gas compositions, however, persist in the ice matrix, and in isolated pockets or melt lenses. Precipitation and accumulation rates, seasonal temperatures, and wind all control the proportion of wet deposition firn gas in the total firn column. We speculate that ice cores taken at sites of extremely dry and cold polar conditions with low accumulation rates should produce the best possible transfer and preservation of gases in atmospheric concentrations. Vostok and Taylor Dome sites would appear to minimize factors complicating interpretation of ice gas bubble chemistry. The Greenland GISP2 site presents more of a challenge to interepretation of gas data. Much more research on identifying and quantifying the important transfer processes between atmosphere

and occluded ice bubbles through the firn column is needed. Assumptions in ice core gas studies must be recognized and evaluated.

Future Research Directions

The unusual and controversial shallow firn gas compositions observed in this study have very important implications for interpretation of ice core gas data and deciphering paleoclimate records in ice. These results must be corroborated at other sites, including more temperate regions as in winter snowpack of the high Colorado Rockies. Direct measurement of CO_2 using a portable IR CO_2 analyzer (IRGA) at the snow surface and at depth in regions of high snowfall above 3,600 meters elevation, should document the processes of in-cloud scavenging and solubility-sorption processes suggested here. Elevated CO_2 concentrations that we report are not unprecedented (Coyne and Kelley, 1974; Sommerfeld, Musselman, and others, 1991) in snowpack. Critically important is the documentation with stable isotope measurements of CO_2, the gas variations we report in firn. This work is in progress with the development of an open-split interface to a Finnigan 252 sector mass spectrometer that will enable picomole level stable isotope measurements. We further plan to evaluate the chromatographic effects associated with gas transfer through snow using actual snow-packed columns and standard gas injection into a helium carrier flow while monitoring the effluent with our quadrupole mass spectrometer. However, the most important future research is the use of a laser microbeam sampling system to open individual gas bubbles for analysis on the mass spectrometer. This equipment is discussed in Appendix A. Gas heterogeneity, mixing, and compositional variations between different gas retention sites in ice (bubbles, clathrates, grain boundaries and junctions, micropore voids, and crystal defect sites) can be evaluated. The matrix gas hypothesized in this report can be confirmed in compositional detail. Using this laser system, we plan to investigate the details of compositional changes across the firn-ice transition as permeability drops to essentially zero. With continued compression and recrystallization of the ice at greater depths, we will examine the possible compositional changes in both gases and isotopes. The very high

spatial resolution of a single gas bubble, coupled with stable isotope ice measurements, may permit detailed documentation for addressing the important climate question: "Does buildup of CO_2 greenhouse gases in the atmosphere precede climate warming events, or does warming stimulate a positive feedback carbon dioxide flux increase?"

Acknowledgements

We wish to thank the USGS Global and Climate Change program and the Office of Mineral Resources for continued support during development of this highly specialized equipment and methods. We acknowledge the generous support and enthusiasm of U.S. National Park Service staff in the Wrangell-St. Elias office, especially R. Galipeau and D. Rosencrantz, and the Denali Search and Rescue personnel. R. Dickerson provided indispensible mountaineering and sampling assistance on the Klutlan Glacier and on the ascent of Mt. Churchill and Mt. Bona in the Wrangell-St. Elias range, Alaska. Taylor Dome site studies were facilitated by NSF funding to P. Grootes and E. Waddington of the University of Washington. Logistical support for our work in Greenland and Antarctica was provided by the National Science Foundation. Our activities at Summit were graciously tolerated by the NSF-sponsored Greenland Ice Sheet Project (GISP2). Special thanks are given to A. Gow and B. Elder of CRREL (U.S. Army Cold Regions Research and Engineering Laboratory) for their assistance in sample collection at GISP2. Finally, thanks to the Polar Ice Coring Office/University of Alaska Fairbanks (PICO/UAF) staff who assisted with numerous aspects of field logistics and technical problems. MSA analyses were generously provided by Pai-Yei Whung (Rosensteil Center for Marine and Atmospheric Sciences, University of Miami), and stable isotope data were provided by R. Rye (USGS, Denver).

References Cited

Adamson, A.W., 1982, Physical Chemistry of Surfaces (4th ed.): New York, John Wiley & Sons, 664 p.

Balzers High Vacuum, Inc., 1994, Quadstar 421 Users Guide (2.3.1 ed.): Fürstentum, Liechtenstein, Balzers.

Bender, M.L., Sowers, T., Barnola, J.-M., and Chappellaz, J., 1994, Changes in the O_2/N_2 ratio of the atmosphere during recent decades reflected in the composition of air in the firn at Vostok Station, Antarctica: Geophysical Research Letters, v. 21, no. 3, p. 189-192.

Colbeck, S.C., 1989, Air movement in snow due to windpumping: Journal of Glaciology, v. 35, no. 120, p. 209-213.

Coyne, P.I., and Kelley, J.J., 1974, Variations in carbon dioxide across an Arctic snowpack during spring: Journal of Geophysical Research, v. 79, no. 6, p. 799-802.

Craig, H., Horibe, Y., and Sowers, T., 1988, Gravitational separation of gases and isotopes in polar ice caps: Science, v. 242, p. 1675-1678.

Davidson, C.I., 1989, Mechanisms of wet and dry deposition of atmospheric contaminants to snow surfaces, *in* The Environmental Record in Glaciers and Ice Sheets, The Dahlem Workshop, Berlin, John Wiley & Sons, p. 29-52.

Fitzpatrick, J.J., Hinkley, T.K., Landis, G.P., Rye, R.O., and Holdsworth, G., 1992, High-resolution paleoclimate reconstruction from Alaskan ice-core records, *in* Carter, L.M.H., ed., U.S. Geological Survey Research on Energy Resources, McKelvey Forum 1992, U.S. Geological Survey Circular 1074, p. 29.

Gedzelman, S.D., and Arnold, R., 1994, Modeling the isotopic composition of precipitation: Journal of Geophysical Research, v. 99, no. D5, p. 10455-10471.

Grootes, P.M., Steig, E.J., and Massey, C., 1991, Taylor Ice-Dome Study-- Reconnaissance 1990-1991: Antarctic Journal of the U.S., v. 26, no. 5, p. 69-71.

Grootes, P.M., Stuiver, M., White, J.W.C., Johnson, S., and Jouzel, J., 1993, Comparison of

oxygen isotope records from the GISP2 and GRIP Greenland ice cores: Nature, v. 366, p. 552-554.

Hinkley, T.K., Fitzpatrick, J.J., Landis, G.P., and Rye, R.O., 1991, High-resolution paleoclimate reconstruction from Alaskan ice-core records: Geological Society of America Abstract with Programs, v. 23, p. A352.

Jaworowski, Z., Segalstad, T.V., and Hisdsal, V., 1992, Atmospheric CO_2 and global warming-- A critical review (2nd ed.): Norsk Polarinstitutt, v. Meddelelser Nr. 119, 72 p.

Landis, G.P., Fitzpatrick, J.J., Hinkley, T.K., and Rye, R.O., 1993, Paleoclimate reconstructions from Alaskan ice records-- teleconnections between Pacific-North American (PNA), Reverse PNA, and El Niño-Southern Oscillation (ENSO) states, *in* Kelmelis, J.A., and Snow, M., eds., Proceedings of the U.S. Geological Survey Global Change Research Forum, U.S. Geological Survey Circular 1086, p. 93.

Martinerie, P., Lipenkov, V.Y., Raynaud, D., Chappellaz, J., Barkov, N.I., and Lorius, C., 1994, Air content paleo record in the Vostok ice core (Antarctica)-- A mixed record of climatic and glaciological parameters: Journal of Geophysical Research, v. 99, no. D5, p. 10565-10576.

Martinerie, P., Raynaud, D., Etheridge, D.M., Barnola, J.-M., and Mazaudier, D., 1992, Physical and climatic parameters which influence the air content in polar ice: Earth and Planetary Science Letters, v. 112, p. 1-13.

Nakazawa, T., Machida, T., Esumi, K., Tanaka, M., Fujii, Y., Aoki, S., and Watanabe, O., 1993, Measurements of CO_2 and CH_4 concentrations in air in a polar ice core: Journal of Glaciology, v. 39, no. 132, p. 209-215.

Schwander, J., 1989, The transformation of snow to ice and the occlusion of gases, *in* The Environmental Record in Glaciers and Ice Sheets, The Dahlem Workshop: Berlin, John Wiley & Sons, p. 53-68.

Schwander, J., Barnola, J.-M., Andrié, C., Leuenberger, M., Ludin, A., Raynaud, D., and Stauffer, B., 1993, The age of the air in the firn and the ice at Summit, Greenland: Journal

of Geophysical Research, v. 98, no. D2, p. 2831-2838.

Sommerfeld, R.A., Musselman, R.C., Reuss, J.O., and Mosier, A.R., 1991, Preliminary measurements of CO_2 in melting snow: Geophysical Research Letters, v. 18, no. 7, p. 1225-1228.

Sowers, T., Bender, M., and Raynaud, D., 1989, Elemental and isotopic composition of occluded O_2 and N_2 in polar ice: Journal of Geophysical Research, v. 94, no. D4, p. 5137-5150.

Stauffer, B., Neftel, A., Oeschger, H., and Schwander, J., 1985, CO_2 concentration in air extracted from Greenland ice samples, *in* Langway, C.C., Jr., Oeschger, H., and Dansgaard, W., eds., Greenland Ice Core: Geophysics, Geochemistry, and the Environment: American Geophysical Union, p. 85-89.

Waddington, E.D., Morse, D.L., Balise, M.J., and Firestone, J.F., 1991, Glacier geophysical studies for an ice core site at Taylor Dome: Antarctic Journal of the U.S., v. 26, no. 5, p. 71-73.

Wahlen, M., Allen, D., and Deck, B., 1991, Initial measurements of CO_2 concentrations (1530 to 1940 AD) in air occluded in the GISP2 ice core from central Greenland: Geophysical Research Letters, v. 18, no. 8, p. 1457-1460.

Wilhelm, E., Rattino, R., and Wilcock, R.J., 1977, Low-pressure solubility of gases in liquid water: Chemical Reviews, v. 77, no. 2, p. 219-262.

Zumbrunn, R., Neftel, A., and Oeschger, H., 1982, CO_2 measurements on 1-cm^3 ice samples with an IR laserspectrometer (IRLS) combined with a new dry extraction device: Earth and Planetary Science Letters, v. 60, p. 318-324.

Appendix A
Analytical Methods and Calibration

Instrumental Configuration—- All firn gas analyses were performed using a Balzers Model 421-5 quadrupole mass spectrometer (QMS) mounted within a custom fabricated vacuum system. The QMS utilizes 30 cm rods of 16 mm diameter and operates with an rf frequency tuned for a mass range of 0-334 AMU. This quadrupole mass spectrometer was selected for its increased stability and improved resolution. Typical mass resolution to ± 1/64 AMU is maintained for >24 hours. A partial pressure detection limit 2x background is 10^{-15} of total pressure, making ppm and ppb level measurements on very small samples possible. Scan rates across masses can be set as fast as 100 microseconds per mass unit which permits rapid determination of a large number of 12-bit intensities and improved measurement statistics. Instrument control, data acquisition and reduction utilized the proprietary software Quadstar v2.3.1 distributed by Balzers (Balzers, 1994). This configuration enabled high-speed real-time data collection and reduction to concentration data via a fiber optic cable interface to the 486DX266 Windows-based computer. Figure A1 illustrates the important aspects of this design, as well as noted provisions for additional features of this instrumentation presently under development. The mass spectrometer utilizes an open cross-beam ion source with vacuum mounted collimating source magnets and thoriated iridium filaments. A gas tight axial beam ion source is planned for future installation to improve an already low background on the carbon dioxide mass 44 (presently at mid-10^{-12} amps). Emission was set at 0.8 milliamps. Ion detection was via a 17-stage dynode secondary electron multiplier (SEM) operated at 2200 vDC with gain calibration established by use of a computer-selected separate faraday cup collector and electrometer circuitry. Standby background vacuum of < 10^{-10} torr was achieved in the mass spectrometer chamber with a 240 l/s turbomolecular pump. A 60 l/s turbomolecular pump on the sample inlet manifold produced a similar "blank" vacuum of <10^{-9} torr. Gas samples were admitted into the source region of the mass spectrometer with a thermo-regulated leak

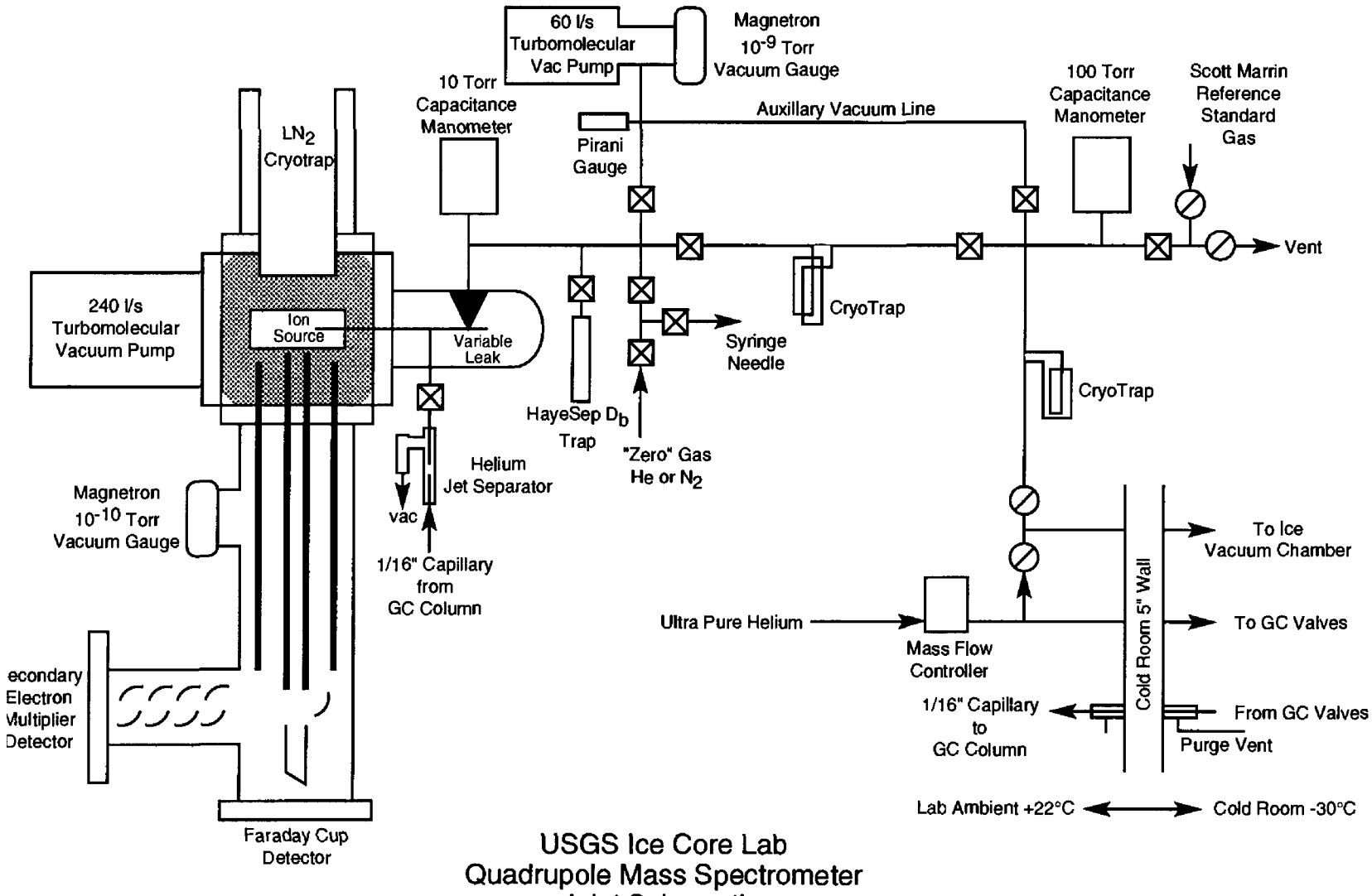

USGS Ice Core Lab
Quadrupole Mass Spectrometer
Inlet Schematic

Figure A1. Schematic block diagram of USGS Balzers 421-5 quadrupole mass spectrometer system.

valve. Pressures in the quadrupole mass spectrometer chamber were approximately 2 x 10^{-7} torr during analysis. A constant leak pressure during analysis was maintained to better than 1 tenth, in spite of 3-5°C temperature drifts in the laboratory. Vacuum valves are positioned for introduction of NIST traceable "air" reference gas and other calibration gases, and a gas syringe needle is valved for sampling the gas contained in the vacutainer vials. All valves are bakeable, all-metal, high-vacuum valves in critical positions, or Kel-f tipped diaphragm metal gasketed valves in less critical positions. Manifold vacuum and sample size are monitored by capacitance manometer transducers, and magnetron "cold cathode" gauges measure high vacuum conditions. During the analysis, the magnetron vacuum gauge mounted in the mass spectrometer chamber was switched off to avoid serious ion reactions in the sample gas. Typical analyses can be accomplished in approximately 15 minutes.

The mass spectrometer inlet design includes additional features for operations other than firn gas analysis. The quadrupole mass spectrometer system is positioned in the laboratory against the wall of a small walk-in 6' x 10' cold room kept at -30°C in which is placed a custom microscope with zinc selenide optics. The microscope is optically coupled through mirrors and

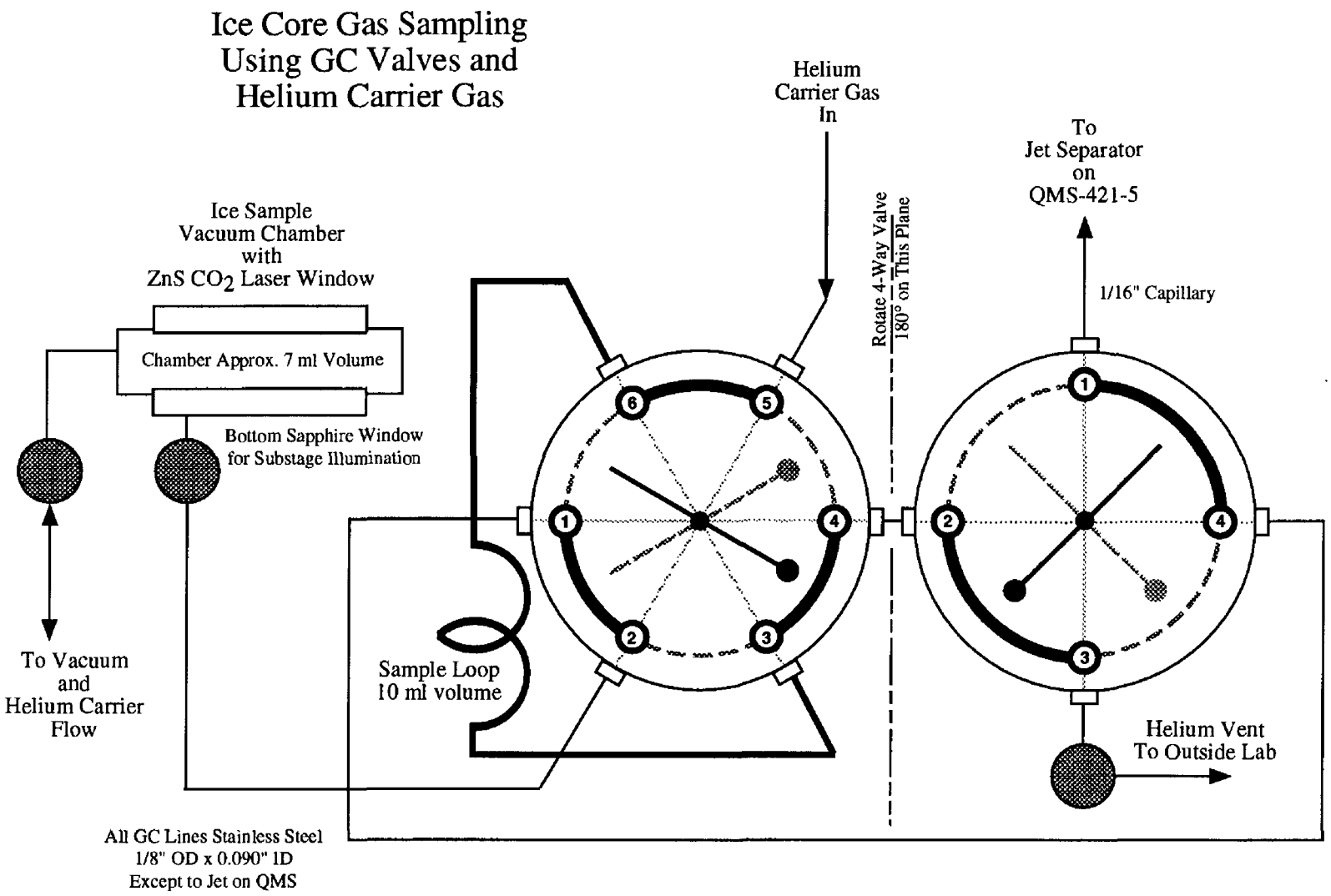

Figure A2. Schematic of Valco gas chromatography valves and connections to the ice chamber mounted on a zinc selenide carbon dioxide gas laser microscope system. The valves and ice chamber enable placing the ice section under vacuum, at helium partial pressure, or in a regulated helium flow. Both head space gases can be sampled and direct flow injection while firing the laser beam to open individual gas bubbles. Indicated connections pass through the cold room wall to the quadrupole mass spectrometer system as in figure A1.

windows to a 25 watt carbon dioxide gas laser in the laboratory that produces a 60-100 μ diameter beam focused through a ZnS vacuum window to an ice section positioned on the microscope stage in a vacuum chamber. The stage is remotely operated with indexed servo-motors to provide x-y-z positioning while viewing the section through a high resolution (525 line) CCD camera. Ambient lab temperature is approximately 22°C, whereas the cold room temperature is maintained at -30°C. All final sample handling and section preparation can be

completed in the cold room laboratory equipped with emery sheets, a hot plate, and binocular microscope. The CO_2 laser has a co-axial HeNe laser for aiming, and post-video contrast image enhancing circuitry that can generate a synthetic cross-hair for aiming. This equipment allows opening of individual gas bubbles in ice sections by microbeam melting of the ice and handling of released gas for analysis by the quadrupole mass spectrometer. Gas chromatograph VALCO multiport valves (fig. A2) and ultra-pure helium are connected to the vacuum chamber and brought back out through the wall of the cold room with the main vacuum line to the inlet system.

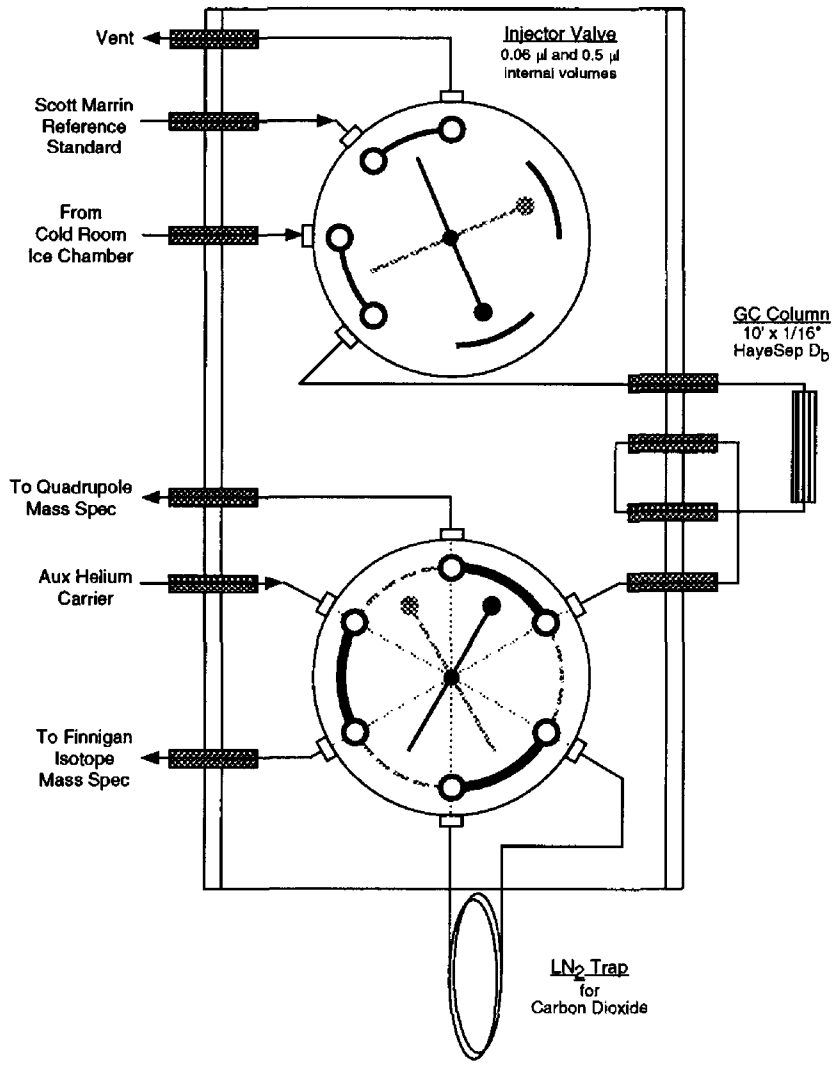

Figure A3. Valco capillary GC valves mounted outside cold room to direct ice core gases through a GC column and either to the jet separator inlet on quadrupole mass spectrometer, or to the open split interface of a Finnigan 252 mass spectrometer for stable isotope analysis of CO_2 or N_2 gas. Standard gas injector valve is configured with volumes comparable to amount of gas from a 1 mm (0.5 µl) or a 0.5 mm (0.06 µl) diameter ice core bubble. Cryofocusing of carbon dioxide prior to transfer to open split interface is possible with trap.

Gas mixtures from the ice section can be directed through a simple 10 foot length of 1/16" packed column (fig. A3) for chromatographic separation of gases prior to introduction into the mass spectrometer through a separate helium jet separator port. This jet separator removes ≈ 95 percent of the helium flow from the sample before injection into the mass spectrometer. Helium flow is controlled using an MKS helium flow controller with a range of 1-50 sccm/min Helium. Helium is research grade tank gas which is passed through an ASCARITE II cylinder, and a drierite and molecular sieve trap prior to entering the flow controller. The gas released in the vacuum chamber can be handled using ultra-pure helium carrier gas and flow injection methods, and using a cryosorption trap to 'focus' the released gas in front of the mass spectrometer leak valve. With both methods, a single gas bubble,

approximately 200-500 μ in diameter, yields sufficient gas for analysis (typically 0.02-0.06 μl STP or less). Ongoing development of this method and results from application to ice core studies will be reported elsewhere.

Firn gas samples in vacutainers are expanded into the small volume (≈20 cm^3) in front of the leak valve by first partially penetrating the vacutainer septum with the gas syringe needle, pumping to the tip of the needle to obtain a vacuum of approximately 2 x 10^{-6} torr, then closing the vacuum port valve and completely puncturing the septum and releasing the sample firn gas into the volume. The sample is allowed to equilibrate for 4 minutes before the needle port is closed and the vacutainer vial is retracted from the needle. At that point, sample gas is leaked into the mass spectrometer to a predetermined signal intensity of 1 x 10^{-6} amps an mass 28. The sample gas is then analyzed by the procedures outlined below.

Calibration and Conditions for Analysis— Quantitative analysis of larger firn gas samples (≈ 8 ml STP) can be conducted through the leak valve after calibration of the instrument. Routine calibration is performed several times per day using a synthetic air sample of NIST traceable composition as explained below. Prior to analysis, a mass scale correction is determined, a 'zero' gas background is measured, and the electrometer baseline offset is determined for correcting measured intensities at each of the selected masses. At the beginning of the analysis session, the high vacuum QMS chamber magnetron is turned off to avoid serious gas reactions in the sample that produce N_2O at mass 44 from reaction of N_2 and O_2 that cannot be discriminated from CO_2 at the same mass (fig. A4).

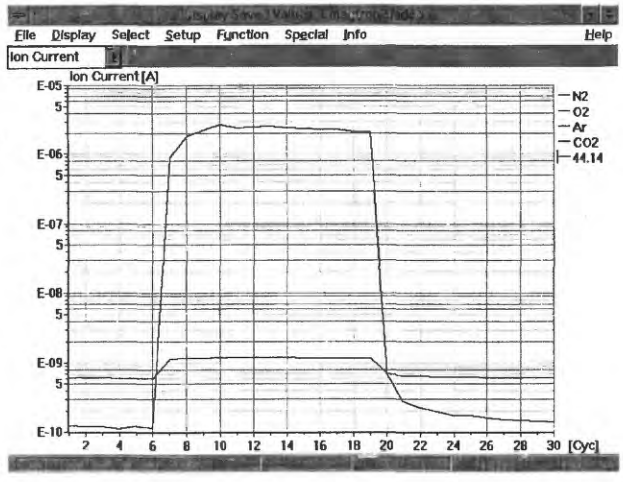

Figure A4. Intensity trace of mass 44 (smaller signal) and of CO_2 concentration (larger signal) in response to switching on and off the magnetron vacuum gauge. N_2 and O_2 react to produce N_2O at mass 44 in the plasma of the cold cathode gauge yielding spurious carbon dioxide values.

The electrometer zero offset is determined by measuring the output at an AMU of 5.5,

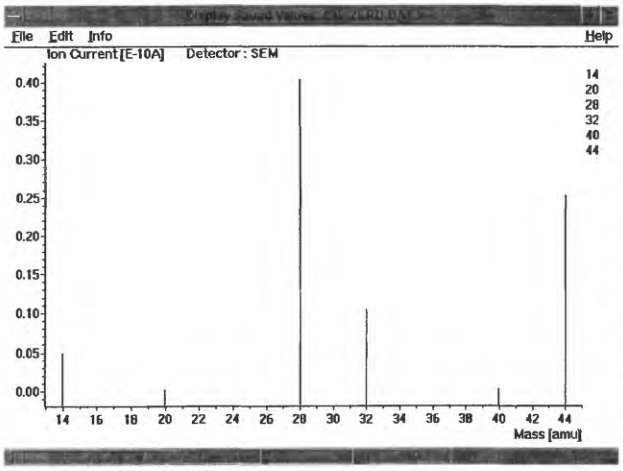

Figure A5. Zero gas helium background mass spectrum which is subtracted from measured intensities.

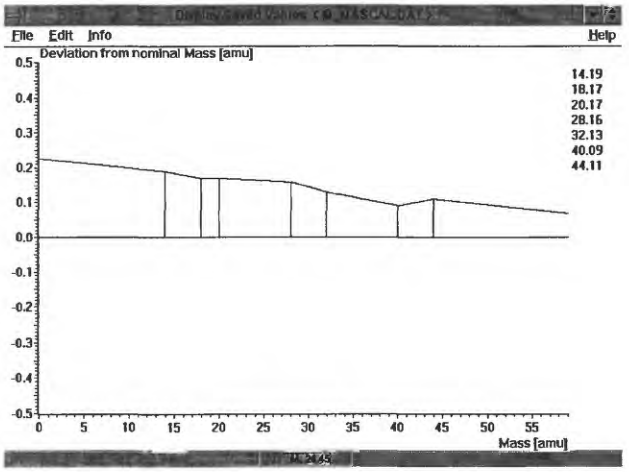

Figure A6. Mass scale calibration for maximum peak intensity as offset from nominal mass units.

which has no contributing mass fragments. The offset correction is applied to all other mass intensity measurements. Background subtraction is determined by use of a "zero" gas which is introduced at the same pressure through the same flow path as the sample to the mass spectrometer, but which does not contribute to the masses of interest (fig. A5). Either ultra-pure helium or dry nitrogen head space gas from a liquid nitrogen storage tank is used. Nitrogen background peaks are 10^{-5} to 10^{-6} of the sample intensities so any small background correction can be used for nitrogen while still obtaining valid measurements of background contributions to other mass intensities. Also, use of nitrogen as a "zero" gas gives the best approximation to an actual sample as it is a near identical matrix for ionization of air gas components. The "zero" gas background is preferred over using the ultimate pumpdown high vacuum background conditions because "zero" gas flow at the pressure of analysis causes desorption from the walls of the vacuum apparatus and more accurately represents spurious contributions to the sample intensity measurements. Accurate quantitative analyses require that intensities be determined at the peak maximum in peak jump operations. All nominal selections of AMU to measure ion intensities must first be corrected for maximum peak intensities in fractional mass units. Calibration of the mass scale is only approximately linear and is determined empirically. Mass resolution is $1/64^{th}$ of an AMU. The span and zero of the rf generator are adjusted to yield mass scale corrections 0.1 to 0.2 AMU larger than the nominal mass specification (fig. A6).

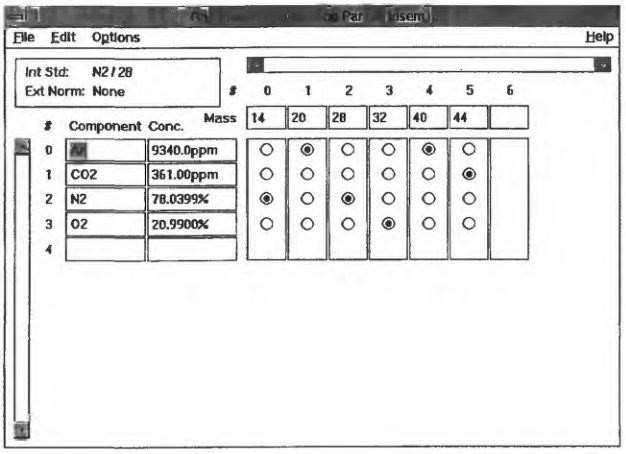

Figure A7. Selected calibration matrix set for specific gas composition.

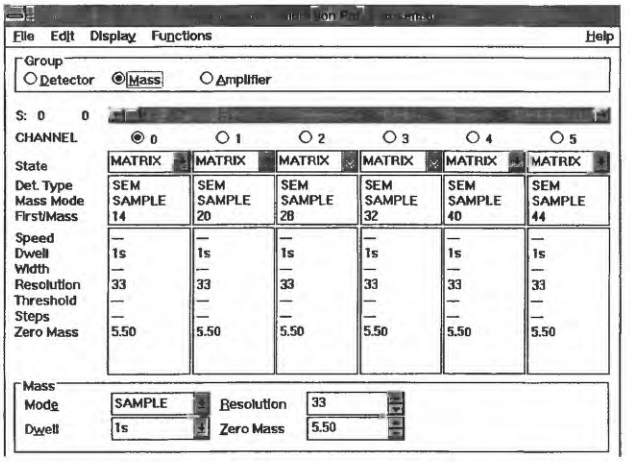

Figure A8. Mass parameter file.

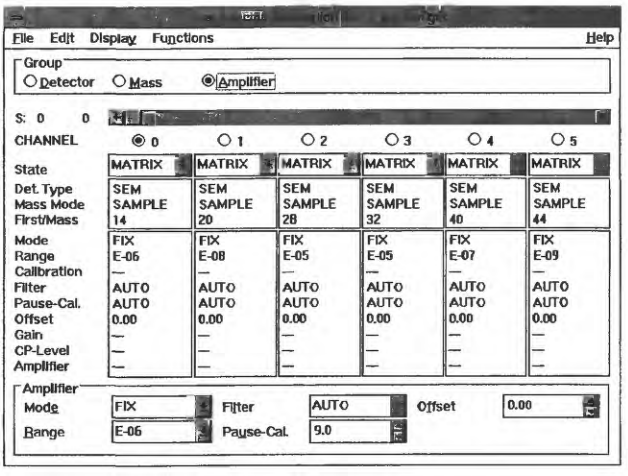

Figure A9. Amplifier parameter file.

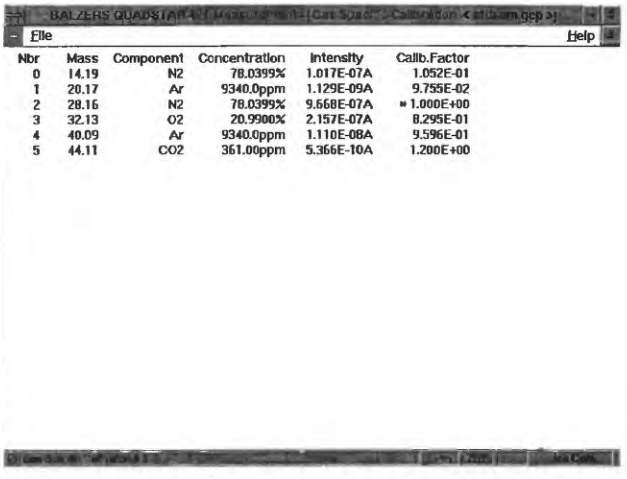

Figure A10. Calibration factor results of specific gas calibration using Scott-Marrin reference air.

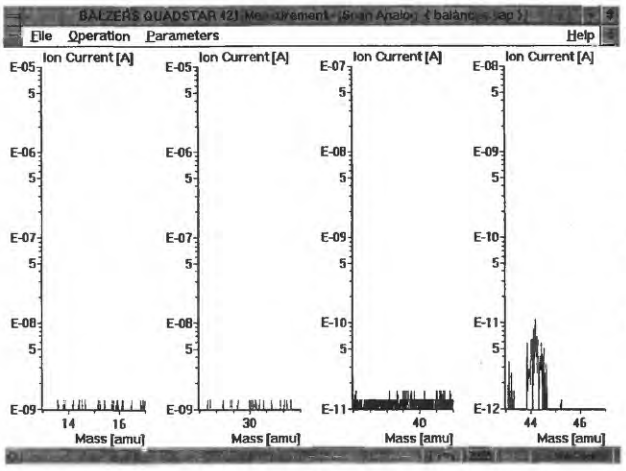

Figure A11 a. Background on inlet balance spectra.

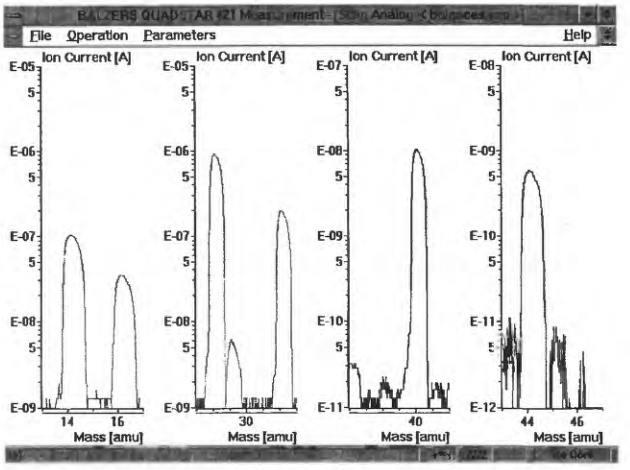

Figure A11 b. Full sample signal on inlet balance spectra with sample set to 10^{-6} amps on mass 28.

Calibration of the instrument involves use of a reference standard air of known composition upon which the mass spectrometer response can be determined. The relationship is established Concentration = (Intensity)/(Calibration Factor) for each mass intensity related to each gas species. Figure A7 illustrates the matrix of selected mass units and specified composition of our standard reference, a synthesized air cylinder from Scott-Marrin, Inc. Figures A8 and A9 illustrate the measurement parameters optimized for this calibration. In this manner the calibration factors are determined (fig. A10) and normalized to AMU=28 of nitrogen. Though we perform sample gas measurements under near identical instrumental conditions, normalization makes the measurement sequence insensitive to minor changes in gas flow or ion source pressure. Sample or standard gas is introduced to the mass spectrometer (fig. A11a and A11b) by adjusting the nominal intensity of AMU 28 (nitrogen) to 1 x 10^{-6} amps. Short term (5 minutes after previous analysis) background and sample mass spectra indicate the presence only of the known air gases of interest (fig. A12a and A12b), with the exception of minor H_2O and H_2 trace gases at AMU 17, 18, and 2. Matrix reduction and calculation of the composition in concentration units is processed in real-time, displayed, and stored to a file. Figure A13 shows an argon trace through a 20 cycle measurement sequence, and figure A14 shows the concentration (in ppmV) of carbon dioxide over 30 cycles. The analytical results do not exhibit significant drift.

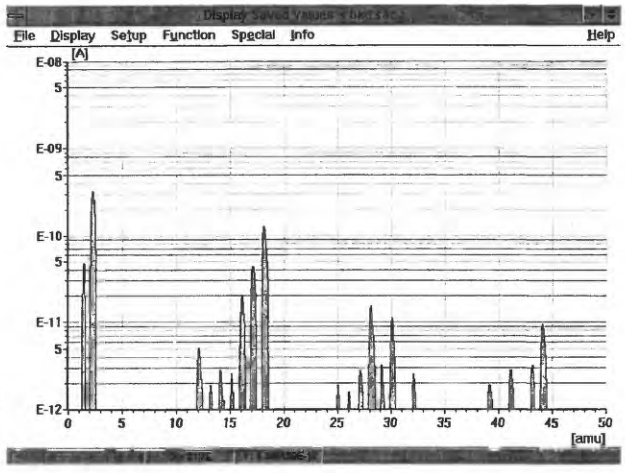

Figure A12 a. Background spectrum. Only 'air' and H_2-H_2O peaks are present. Mass 44 ≈ 10^{-12}amp.

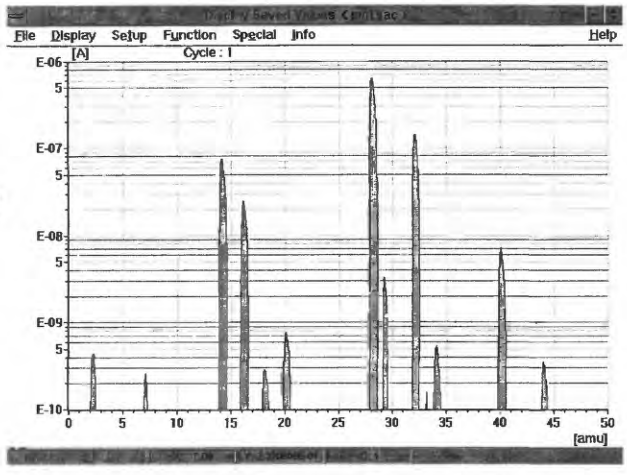

Figure A12 b. Sample mass spectrum at close to analytical operating pressure.

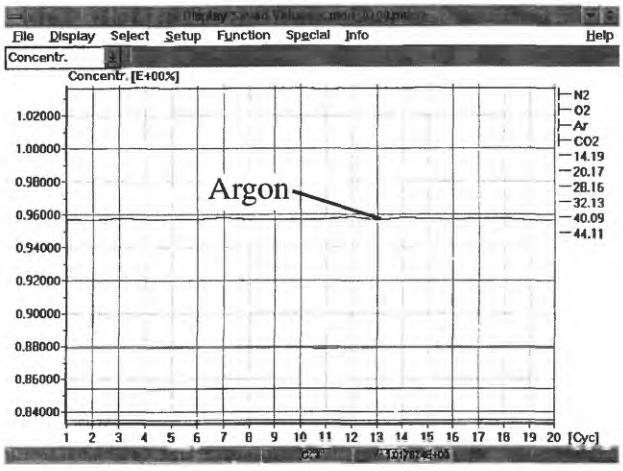

Figure A13. Argon concentration trace.

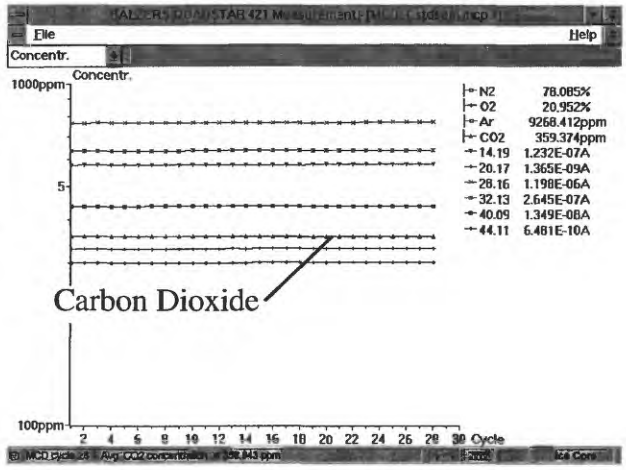

Figure A14. Time trace of intensities and CO_2 concentration. Other species are offscale.

Calibration specifications— To verify the calibration procedures the standard reference gas (Scott-Marrin) air and three other reference gases of certified carbon dioxide composition were analyzed (table A1). These analyses are plotted as CO_2 certified versus CO_2 measured (fig. A15). Over a range of CO_2 from 101 ppmV to 1011 ppmV, the regression slope is 1.007. Twenty-five repeat analysis (table A2) of the Scott-Marrin standard over 2 1/2 months yields the following analytical one sigma precision N_2 = 78.071 ± 0.015; O_2 = 20.968 ± 0.014; Ar = 9255 ± 17.6 ppm; and CO_2 358.7 ± 0.72 ppm.

Table A1. Quadrupole mass spectrometer carbon dioxide calibration data and reference standards.

Reference Name	n meas	Nitrogen percent	Oxygen percent	Argon ppm	Measured CO_2 ppm	Certified CO_2 ppm
Scott-Marrin Std0019	30	78.0130 ±6.572e-03	21.0284 ±7.927e-03	9226.6 ±22.30	359.57 ±0.674	361 ±3.6
Scotty 101	20	99.9899 ±3.034e-05	----	----	100.72 ±0.291	101 ±2.0
Scotty 408	20	99.9589 ±5.039e-05	----	----	411.18 ±0.506	408 ±8.2
Scotty 1011	20	99.8995 ±7.810e-05	----	----	1005.20 ±0.787	1011 ±20.2
Scott-Marrin Std0020	20	78.0737 ±7.098e-03	20.9584 ±7.726e-03	9317.9 ±10.58	360.44 ±0.642	361 ±3.6
Scott-Marrin Std0021	20	78.0882 ±5.534e-03	20.9521 ±5.868e-03	9237.2 ±26.21	360.22 ±0.817	361 ±3.6
Scott-Marrin Certification	----	78.0399 ±0.78	20.9900 ±0.21	9340 ±93.4	361 ±3.6	----

Scott-Marrin Reference Standard "Air" is Cylinder No. CC121990, NIST traceable certified 6/9/93 at ± 1% analytical accuracy (Scott-Marrin, Inc., 6531 Box Springs Blvd., Riverside, CA 92507). Scotty reference cylinders are certified carbon dioxide in nitrogen Scotty II cylinders (Scott Speciality Gases, 500 Weaver Park Road, Longmont, CO 80501). Scotty 101 is Can Lot 205 (A-8242), Scotty 408 is Can Lot 46 (K-015866), and Scotty 1011 is Can Lot 498 (A-5420). All Scotty II gas mixtures are ± 2% analytical accuracy. Below each analysis is 1 standard deviation based upon the n measurements indicated.

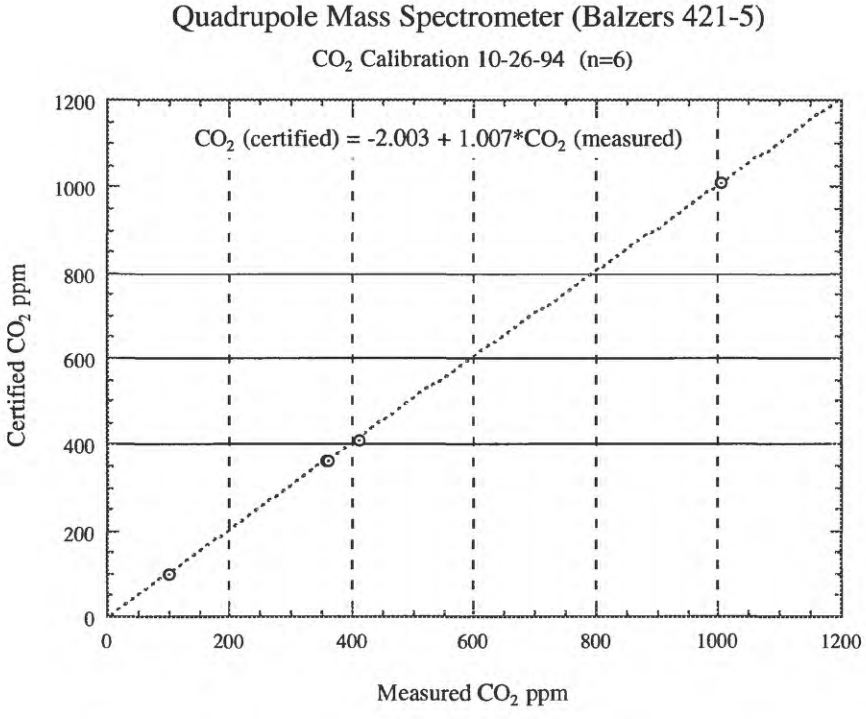

Figure A15. Plot of certified versus measured carbon dioxide content in standard gas listed in table A1.

Table A2. Scott-Marrin Standard Reference Air: Repeat Analysis

File	Date	N2	N2 Sigma	O2	O2 Sigma	Ar	Ar Sigma	CO2	CO2 Sigma
Std00017	26-Oct-94	78.1066	0.0110	20.9	0.0111	9247.1	5.9	359.0	0.83
Std00018	26-Oct-94	78.0578	0.0040	20.9833	0.0043	9229.6	13.9	359.1	0.55
Std00019	26-Oct-94	78.0130	0.0066	21.0284	0.0079	9 5.6	22.3	359.6	0.67
Std00020	26-Oct-94	78.0737	0.0071	20.9584	0.0077	9317.9	10.6	360.4	0.64
Std00021	26-Oct-94	78.0882	0.0055	20.9521	0.0059	9237.2	26.2	360.2	0.82
StdA0022	9-Nov-94	78.0478	0.0063	20.9874	0.0062	9290.2	33.2	358.2	0.53
StdB0022	9-Nov-94	78.0420	0.0075	20 36	0.0072	9285.0	4.8	358.8	0.56
Std00023	10-Nov-94	78.0543	0.0037	20	0.0036	9284	3.4	359.0	0.53
Std00025	17-Nov-94	78.1146	0.0161	20.9 9	0.0143	9226.7	18.7	358.3	0.51
Std00027	28-Nov-94	78.1515	0.0466	20.8916	0.0432	9211.0	34.5	358.0	0.70
Std00030	29-Nov-94	78.1057	0.0142	20.9357	0.0134	9227.4	8.8	358.2	0.38
Std00031	30-Nov-94	78.0063	0.0071	21.0259	0.0070	9318.7	4.3	359.1	0.44
Std00032	30-Nov-94	78.0152	0.0107	21.0177	0.0099	9312.6	8.4	359.0	0.73
Std00035	27-Dec-94	78.0580	0.0125	20.9 7	0.0106	9233.5	22.4	358.8	0.61
Std00036	27-Dec-94	78.0519	0.0206	20.9 5	0.0187	9279.8	19.8	357.9	0.55
Std00037	27-Dec-94	78.1570	0.0241	20.8854	0.0215	9220.2	25.6	356.4	0.60
Std00038	28-Dec-94	78.0584	0.0155	20.9836	0.0144	9221.4	12.8	358.4	0.34
Std00039	30-Dec-94	78.1365	0.0452	20.9076	0.0404	9201.7	47.6	356.8	1.26
Std00040	5-Jan-95	78.0817	0.0110	20.9841	0.0084	9184.7	29.5	357.9	0.59
Std00041	5-Jan-95	78.1031	0.0421	20.9 7	0.0371	9206.4	49.2	355.9	1.95
Std00043	6-Jan-95	78.0 4	0.0161	21.0 2	0.0157	9276.2	18.0	358.1	0.50
Std00044	6-Jan-95	78.0725	0.0163	20.9614	0.0165	9303.3	6.3	357.6	0.90
Std00045	9-Jan-95	78.0701	0.0035	20.9708	0.0035	9230.4	4.1	360.9	0.55
Std00046	10-Jan-95	78.0270	0.0075	21.0023	0.0071	9346.1	4.8	360.2	0.74
Std00047	10-Jan-95	78.0 45	0.0061	20.9732	0.0058	9262.0	4.5	361.2	0.93
Average		**78.0711**	**0.0147**	**20.9675**	**0.0137**	**9255.2**	**17.6**	**359.7**	**0.72**

Appendix B
Sequencer Application for Routine Calibration and Analysis

Standardized Analytical Sequence— Quadstar software provides a programming tool for developing custom dialog boxes and control of the sequence of analysis. Table B1 is a sequence program developed for routine analysis that handles all pre-configured analytical parameters and a standardized method for calibration and data acquisition. This software tool enables an inexperienced operator to quickly master routine analyses.

Table B1. Sequencer File For Automation of Routine Calibration and Analysis

QMS 421-5 Quadrupole Mass Spectrometer
Balzers Quadstar v2.1.3 Software

Written by G.P. Landis
January 23, 1995

STANDARD.SEQ

```
// Routine Analysis
SetPar( AlarmDisp=off, AlarmError=off, BarWidth=15, ColorMode=multi, Cycles=20,   DispOpt=last,
LineType=solid, Marker=on, MSC=on, NorMode=sum100,    RelVal=sum100, RollAxis=on, Scale=log,
XLetter=on, XRaster=on, XScale=cycle,      YRaster=on, ZeroEq=on, ZeroSub=on, ScanArran=horiz )
WhileVar( i[2]>=0 )
Begin
        Dialog( Box="Analytical Functions";200;200;400;200, ReturnVar=i[2],
            EnterVal=0,EscapeVal=-1, Button="Balance Inlet";130;140;140;35;1,
            Button="MSC:Mass Scale";220;50;160;35;4, Button="GSC: Reference Gas";
            20;50;190;35;3,Button="Analyze";20;140;100;35;2,
            Button="Exit";280;140;100;35;-1,Text="Calibration Procedures....";
            100;15;205;25, Text="Analysis of Gas-Reference Sample....";
            60;100;300;25 )
        IfVar( i[2]=1 )
                Sequence( Par="c:\qs421\par\balance.seq" )
        IfVar( i[2]=2 )
                Sequence( Par="c:\qs421\par\analyze.seq" )
        IfVar( i[2]=3 )
                Sequence( Par="c:\qs421\par\calibr.seq" )
        IfVar( i[2]=4 )
                Sequence( Par="c:\qs421\par\mass.seq" )
        IfVar( i[2]=0 )
                Message( Text="Make A Selection" )
End
Exit( )
```

BALANCE.SEQ

```
//Set Balance on Inlet SubSequence
WhileVar( i[1]>=0 )
Begin
        Dialog( Box="Pressure Balance Cycles";200;200;390;60, ReturnVar=i[1],
            EnterVal=0,EscapeVal=-1, Text="Enter No. of Scan Cycles 0    10";
            20;20;250;20,Edit=280;15;100;30;i[4] )
        IfVar( i[4]>0 )
                Loop( i[0]=1;i[4] )
                Begin
                    SetString( gs[0] = "Pressure Adjust Scan Cycle @ of @ Total";i[0] )
                    Message( Text=gs[0];i[4] )
                    ScanAnalog( Par="c:\qs421\par\balances.sap" )
                End
        IfVar( i[4]=0 )
                SetVar( i[1]=-1 )
End
```

MASS.SEQ

```
// Mass Scale Calibration SubSequence
InitDisp( )
Message( Text="" )
WhileVar( i[0]>=0, Disp=off )
Begin
        Dialog( Box="Mass Scale Calibration";200;200;370;140, ReturnVar=i[0],
            EnterVal=0,EscapeVal=-1, Button="Calibrate";110;20;150;40;1,
            Button="Calibration Complete (Cancel)";60;80;250;40;-1 )
        IfVar( i[0]=1 )
                MSC( Par="stdsem.msp", CalMode=coarse, Disp=on, SaveMode=reset )
        IfVar( i[0]=0 )
                Message( Text="Please Select a Button" )
End
```

ANALYZE.SEQ

```
InitDisp( )
SetVar( i[0]=0 )
SetVar( i[1]=0 )
WhileVar( i[1]<=5 )
Begin
        SetVar( i[4]=0 )
        Dialog( Box="MCD Mode Selection";200;200;420;280, ReturnVar=i[1],
            EnterVal=0,EscapeVal=10, Text="Select Display Format";120;20;180;20,
            Button="TimeSeries";40;60;100;40;3, Button="BarGraph";160;60;100;40;2,
            Button="Table";280;60;100;40;1, Text="Enter No. of Cycles 1.....40";
            100;120;220;20,Edit=185;160;50;30;i[4], Button="Cancel Measurement";
            40;210;200;40;10,Button="Save Data";280;210;100;40;4 )
        IfVar( i[4]=0 )
```

```
Begin
        IfVar( i[1]=10 )
            Message( Text="Goodbye", Delay=2 )
        Else
        Begin
            Message( Text="You must specify the number of cycles" )
            SetVar( i[1]=5 )
        End
End

IfVar( i[1]=0 )
        Message( Text="Please Select a Button" )
IfVar( i[1]=1 )
        SetDefault( Disp=tab )
IfVar( i[1]=2 )
        SetDefault( Disp=bar )
IfVar( i[1]=3 )
        SetDefault( Disp=vt )
IfVar( i[1]<=3 )

Begin
        IfVar( i[1]>0 )
        Begin
            SetPar( Cycles=i[4] )
            Loop( i[0]=1;i[4] )
            Begin
                    IfVar( i[0]=1 )
                    Begin
                            SetVar( f[0]=0 )
                            SetVar( f[1]=0 )
                    End
                    MCD( Par="stdsem.mcp", SaveGfa=0 )
                    SetString( gs[0] = "MCD cycle @ — Avg.
                        CO2 concentration  = @ ppm";i[0] )
                    Calculate( f[0] = 10000.*gfa[0][3] )
                    Calculate( f[1] = f[1]+f[0] )
                    Calculate( f[2] = f[1]/i[0] )
                    Message( Text=gs[0];f[2] )
            End
        End
End

IfVar( i[1]=4 )
Begin
        SetPar( Cycles=i[4] )
        Dialog( Box="Save File Attributes";200;180;380;200, ReturnVar=i[3],
            EnterVal=0, EscapeVal=-1, Edit=20;75;250;30;gs[1],
            Text="Enter Save File Name and Optional Vector";20;15;340;20,
            Edit=280;75;80;30;i[2], Text="Total 8 Char. Max.";110;45;150;20,
            Button="Save - Append";30;130;150;30;2,
            Button="Cancel Save";220;130;130;30;-1 )

        IfVar( i[3]>0 )
        Begin
```

```
                Loop( i[0]=1;i[4] )
                Begin
                        IfVar( i[0]=1 )
                        Begin
                                SetVar( f[0]=0 )
                                SetVar( f[1]=0 )
                        End
                        IfVar( i[3]=2 )
                                MCD( Par="c:\qs421\par\stdsem.mcp", Disp=vt, SaveGfa=0,
                                    SaveCyc=gs[1];i[2], ChaSave=on )
                        SetString( gs[0] = "MCD cycle @ — Avg.
                                    CO2 concentration  = @ ppm";i[0] )
                        Calculate( f[0] = 10000.*gfa[0][3] )
                        Calculate( f[1] = f[1]+f[0] )
                        Calculate( f[2] = f[1]/i[0] )
                        Message( Text=gs[0];f[2] )
                End
            End
        End
End
```

CALIBR.SEQ

```
// GSC Specific Calibration SubSequence
Message( Text="Start Gas Specific Calibration on Scott Marrin Tank
        Reference Gas" )
InitDisp( )
SetVar( i[0]=0 )
WhileVar( i[0]>=0 )
Begin
    Dialog( Box="Gas Specific Calibration (SM Tank)";200;200;350;80,
        ReturnVar=i[0],EnterVal=1, EscapeVal=-1, Button="Update";
        60;20;100;40;1, Button="Continue";200;20;100;40;-1 )
    IfVar( i[0]>=0 )
        Loop( i[0]=1;5 )
        Begin
            GSC( Par="stdsem.gcp", Disp=on, Prot=off )
            SetString( gs[0] = "Gas Specific Calibration # @";i[0] )
            IfVar( i[0]<5 )
                    Message( Text=gs[0] )
            Else
                    Message( Text=gs[0], Delay=5 )
        End
End
```